

## Using a Tripod as a Chiral Chelating Ligand: Chemical Exchange Between Equivalent Molecular Structures in Palladium Catalysis with 1,1,1-Tris(oxazoliny)ethane (“Trisox”)

Carole Foltz,<sup>[a]</sup> Markus Enders,<sup>[a]</sup> Stéphane Bellemin-Laponnaz,<sup>\*[b]</sup> Hubert Wadepohl,<sup>[a]</sup> and Lutz H. Gade<sup>\*[a]</sup>

Dedicated to Professor Peter Hofmann on the occasion of his 60th birthday

**Abstract:** Threefold symmetrical chiral podands may simplify the stereochemistry of key catalytic intermediates for cases in which they only act as bidentate ligands. This applies to systems in which chemical exchange between the different  $\kappa^2$ -coordinated forms takes place and in which the non-coordinated sidearm may play a direct or indirect role at some earlier or later stage in the catalytic cycle. Palladium(II)-catalysed allylic substitutions provide appropriate test reactions along these lines. A series of neutral dichloropalladium(II) complexes, [PdCl<sub>2</sub>(*i*Pr-trisox)] (**1a**), [PdCl<sub>2</sub>(Ph-trisox)] (**1b**), [PdCl<sub>2</sub>(Bn-trisox)] (**1c**) and [PdCl<sub>2</sub>(Ind-trisox)] (**1d**) (trisox = 1,1,1-tris(oxazoliny)ethane) were synthesised by reaction of the respective trisox derivative with [PdCl<sub>2</sub>(PhCN)<sub>2</sub>] and characterised inter alia by <sup>15</sup>N NMR spectroscopy. Direct detection of the heteronuclei without isotope enrichment and with “normal” sample concentrations was achieved with the aid of a cryogenically cooled NMR probe on a 600 MHz NMR spectrometer. Whereas the <sup>15</sup>N

nuclei of the coordinated oxazoline rings resonate at  $\delta$  = 160–167 ppm and appear as two singlets due to their diastereotopicity, the signal assigned to the dangling oxazoline “arm” is observed at  $\delta$  = 238–240 ppm. Variable-temperature NMR studies along with a systematic series of magnetisation transfer experiments established exchange between ligating and non-ligating oxazoline rings. Reaction of [Pd(allyl)(cod)]BF<sub>4</sub> (cod = cyclooctadiene) with Ph-trisox in CH<sub>2</sub>Cl<sub>2</sub> gave the corresponding allyl complex **2**, for which fast exchange between the three oxazoline heterocycles as well as between the *exo* and *endo* diastereomers was observed along with a very slow  $\eta^3$ - $\eta^1$ - $\eta^3$  process of the allyl fragment (magnetisation transfer). Palladium(0) complexes were prepared by reaction of trisox derivatives or sidearm-functionalised BOX (BOX = bis(oxazoliny)-

dimethylmethane) ligands with [Pd(nbd)(alkene)] (nbd = norbornadiene, alkene = maleic anhydride or tetracyanoethylene). X-ray diffraction studies of the *i*Pr-trisox and Ph-trisox complexes (**3a** and **3b**) established Y-shaped trigonal planar coordination geometries with the trisox ligand coordinated in a bidentate fashion, whilst the  $\pi$ -coordinated maleic anhydride ligand adopts one of the two possible diastereotopic orientations. As the catalytic test reaction, the allylic alkylation of 1,3-diphenylprop-2-enyl acetate substrate with dimethyl malonate as nucleophile (in the presence of *N,O*-bis(trimethylsilyl)acetamide) was investigated for the trisox derivatives, their BOX analogues, and a series of less symmetric “sidearm” functionalised bisoxazolines. The trisoxazoline-based catalysts generally induce a better enantioselectivity compared to their bisoxazoline analogues and display significant reduction of the induction period as well as rate enhancement.

**Keywords:** asymmetric catalysis • chirality • NMR spectroscopy • palladium • trisoxazolines

[a] C. Foltz, Priv.-Doz. Dr. M. Enders, Prof. Dr. H. Wadepohl, Prof. Dr. L. H. Gade  
Anorganisch-Chemisches Institut, Universität Heidelberg  
Im Neuenheimer Feld 270, 69120 Heidelberg (Germany)  
Fax: (+49) 6221-545609  
E-mail: lutz.gade@uni-hd.de

[b] Dr. S. Bellemin-Laponnaz  
Institut de Chimie, UMR 7177  
Université Louis Pasteur, 4 rue Blaise Pascal  
67000 Strasbourg (France)  
Fax: (+33) 390-24-50-01  
E-mail: bellemin@chimie.u-strasbg.fr

## Introduction

The exploitation of  $C_3$  chirality in the design of chiral stereodirecting ligands for homogeneous catalytic transformations is currently the focus of intense research efforts and considerable conceptual debate.<sup>[1–5]</sup> The most frequently cited line of argument put forward to motivate this approach is based on the homotopicity of the “reactive” coordination sites in octahedral complexes representing intermediates in catalytic cycles (Figure 1).<sup>[1a,3b]</sup> The use of such

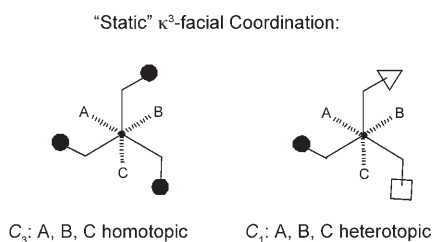


Figure 1. “Static”  $\kappa^3$ -facial coordination of tripod ligands.

symmetrical stereodirecting ligands may reduce the number of transition states and diastereomeric reaction intermediates. In favourable cases, this degeneration of alternative reaction pathways may lead to high stereoselectivity in catalytic reactions and greatly simplifies the analysis of such transformations.<sup>[1,2,6]</sup> Ligand design based on  $C_3$  chirality mostly relates to facially coordinating tripodal ligands. Threefold rotational symmetry represents the only possibility adapted to this topology of ligation, in the same way that  $C_2$  symmetry is related to simple chelation.<sup>[7,8]</sup>

The stereochemical points made above are illustrated for the case of “static”  $\kappa^3$ -facial coordination of a symmetrical chiral tripod in Figure 1. However, a threefold symmetrical chiral podand may generate a similar simplification in the stereochemistry of key catalytic intermediates for cases in which it only acts a bidentate ligand in the stereoselectivity determining step, in other words, for metal complexes with a stereoelectronic preference for non-deltahedral coordination geometries. This is the case for systems in which chemical exchange between the different  $\kappa^2$ -coordinated forms takes place and in which the non-coordinated sidearm may play a direct or indirect role at some earlier or later stage in the catalytic cycle. As is schematically shown in Figure 2, such an exchange represents an equilibrium between identical species for a symmetrical tripod rather than between isomeric complexes, as would be the case for less symmetrical species.

**The test reaction:** We have previously invoked this type of (degenerate) exchange in our interpretation of asymmetric  $Cu^{II}$  catalysed Mannich reactions with prochiral  $\beta$ -ketoesters and related stereoselective transformations with 1,1,1-tris(oxazolanyl)ethane (“trisoX”) derivatives as stereodirecting ligands.<sup>[9,10]</sup> However, the high substitutional lability of the copper(II) complexes along with their paramagnetism pre-

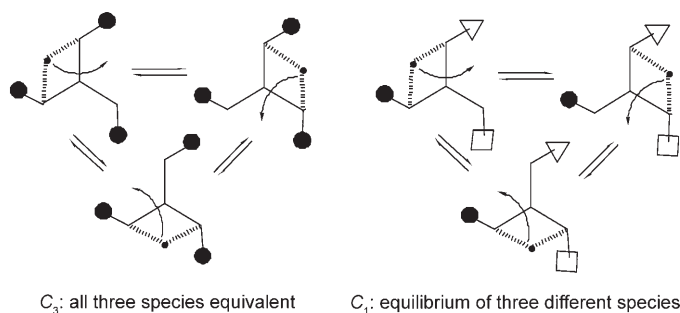
Dynamic Exchange of  $\kappa^2$ -chelated Species

Figure 2. Dynamic exchange of  $\kappa^2$ -chelating tripods coordinated to a complex fragment (●).

cluded a detailed experimental study into this proposed behaviour.<sup>[10]</sup> We therefore decided to study a catalytic reaction that also involves an active species with square planar (i.e. non-deltahedral) coordination geometry, which is diamagnetic and less labile than the  $Cu^{II}$  complexes. Palladium(II)-catalysed allylic substitutions provide appropriate test reactions along these lines and the expected types of interconverting key intermediates (**A**, **B** and **C**) are represented in Figure 3.

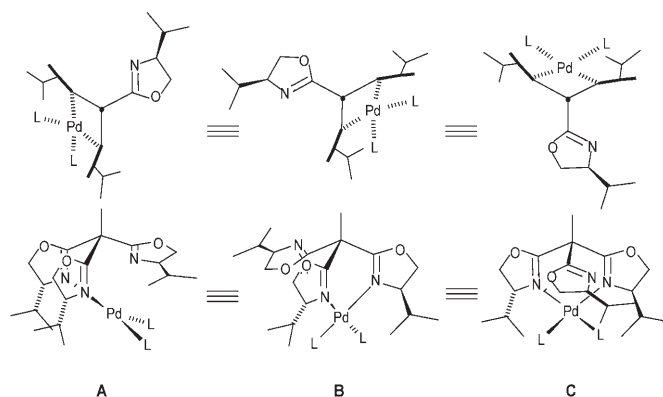


Figure 3. The three symmetry-related square-planar  $Pd^{II}$  complexes bearing  $\kappa^2$ -chelating  $C_3$ -chiral trisoX ligands (top: axial views, bottom: side views).

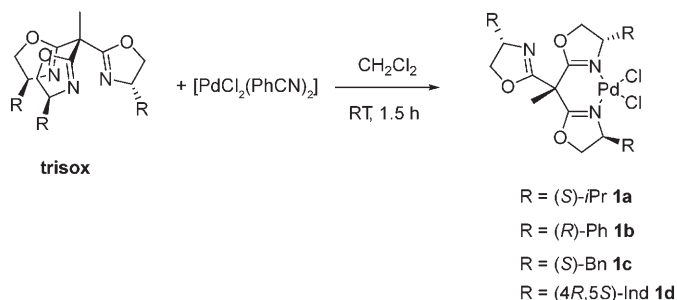
Since the first example of a catalytic asymmetric allylic alkylation in 1977, this process has undergone a considerable development towards a practical synthetic tool.<sup>[11]</sup> New ligands of various types have been developed with numerous substrates and nucleophiles.<sup>[12]</sup> Ligands that have been used successfully in the palladium-catalysed asymmetric allylic alkylation include chiral phosphanes, P,N-chelate ligands or nitrogen-based ligands, such as bisoxazolines.<sup>[13,14]</sup>

This work provides a systematic and comprehensive study into the coordination chemistry of the “trisoX” ligands (trisoX = 1,1,1-tris(oxazolanyl)ethane) with palladium(II) and palladium(0), the dynamic behaviour of the complexes in solution and the use of both symmetrical and non-symmetrical

tripods in palladium-catalysed allylic alkylations. By using various  $C_3$  symmetric trisoxazoline ligands, in addition to bisoxazoline ligands that contain a “hetero”-sidearm,<sup>[15,16]</sup> we demonstrate that the use of potentially tridentate ligands in this reaction results in a rate enhancement and an increase in enantioselectivity relative to corresponding catalysts bearing purely bidentate stereodirecting ligands.

## Results and Discussion

**Synthesis and molecular structures of trisox–palladium(II) complexes:** A series of neutral dichloropalladium(II) complexes was synthesised as depicted in Scheme 1. All four



Scheme 1. Synthesis of palladium(II) complexes **1a–1d**.

complexes,  $[\text{PdCl}_2(i\text{Pr-trisox})]$  (**1a**),  $[\text{PdCl}_2(\text{Ph-trisox})]$  (**1b**),  $[\text{PdCl}_2(\text{Bn-trisox})]$  (**1c**) and  $[\text{PdCl}_2(\text{Ind-trisox})]$  (**1d**) were isolated as crystalline air-stable solids from the reaction of the respective trisox derivative with  $[\text{PdCl}_2(\text{PhCN})_2]$  in  $\text{CH}_2\text{Cl}_2$  at room temperature. Their analytical data confirmed the formulation, and the resonance patterns in the  $^1\text{H}$ ,  $^{13}\text{C}$  and  $^{15}\text{N}$  NMR spectra recorded at 296 K are consistent with a  $\kappa^2$ -coordination of the trisox ligands.

Notably, we obtained good quality  $^{15}\text{N}$  NMR spectra by direct detection of the heteronuclei *without* isotope enrichment and with “normal” sample concentrations with the aid of a cryogenically cooled direct detection probe (Bruker QNP-cryoprobe<sup>TM</sup>, for details see Experimental Section) on a 600 MHz NMR spectrometer. It was possible completely to assign the signals in  $^1\text{H}$  and  $^{13}\text{C}$  NMR spectra of the coordinated oxazolines and the non-coordinated oxazoline by combined 2D  $^1\text{H}$ - $^{15}\text{N}$  and  $^1\text{H}$ - $^{13}\text{C}$  NMR experiments. To our knowledge this is the first such application of  $^{15}\text{N}$  NMR spectroscopy in the coordination chemistry of N-donor ligands. Whereas the  $^{15}\text{N}$  nuclei of the coordinated oxazoline rings resonate at  $\delta = 160\text{--}167$  ppm and appear as two singlets due to their diastereotopicity, the signal assigned to the dangling oxazoline “arm” is observed at  $\delta = 238\text{--}240$  ppm (ext. standard: liquid  $\text{NH}_3$ ). The  $^1\text{H}$ - $^{15}\text{N}$  correlated spectrum of complex **1c** is shown in Figure 4 with the directly recorded one-dimensional  $^{15}\text{N}$  NMR spectrum displayed along the  $F1$  axis. Given the ubiquity of N-donor ligands, we expect this methodology, which is enabled by new spectrometer technology, to find wider applications.

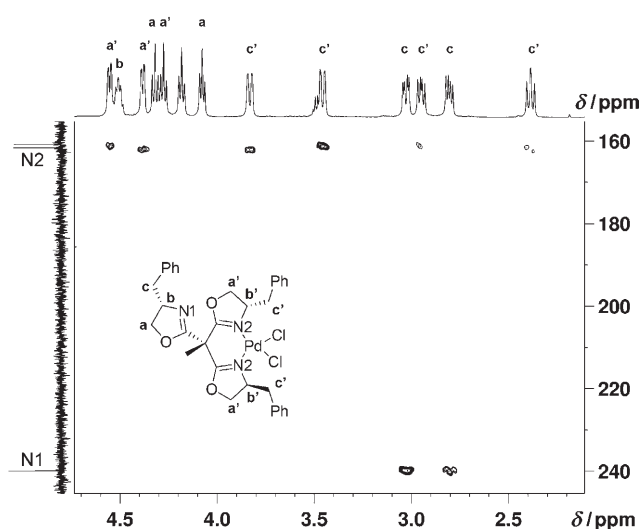


Figure 4. 2D  $^1\text{H}$ - $^{15}\text{N}$  NMR correlated experiment (HMBC) from complex **1c** in  $\text{CDCl}_3$ . The directly recorded one-dimensional  $^{15}\text{N}$  NMR is displayed along the  $F1$  axis.

The molecular structures of the complexes **1a** and **1b** in the solid state are shown in Figures 5 and 6 and with select-

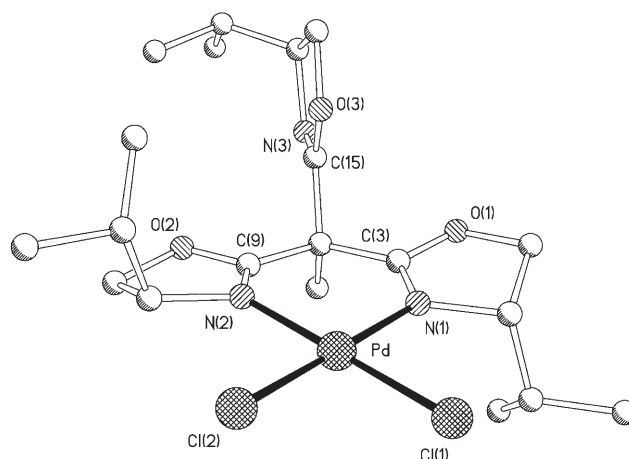


Figure 5. Molecular structure of  $[\text{PdCl}_2(i\text{Pr-trisox})]$  (**1a**). Selected bond lengths (Å) and angles ( $^\circ$ ): Pd–N(1) 2.050(2), Pd–N(2) 2.029(3), Pd–Cl(1) 2.2864(9), Pd–Cl(2) 2.2825(8), N(1)–C(3) 1.272(4), N(2)–C(9) 1.278(4), N(3)–C(15) 1.256(4); Cl(1)–Pd–N(1) 92.31(8), N(1)–Pd–N(2) 88.7(1), N(2)–Pd–Cl(2) 91.84(8), Cl(2)–Pd–Cl(1) 87.09(4).

ed bond lengths and angles given in the figure legend. In both complexes the geometry around the metal centre is distorted square planar, and this deformation is probably a result of steric repulsion between chloro ligands and the isopropyl and phenyl substituents, respectively, of the oxazoline rings.

The trisox ligands adopt bidentate coordination, with the third oxazoline unit dangling, and the N-donor pointing away from the metal centre. The Pd–N and Pd–Cl bond lengths are in the range of those found for related structures.<sup>[17]</sup> As expected, the C=N bond length of the free oxazoline is slightly shorter than those in the coordinated oxa-

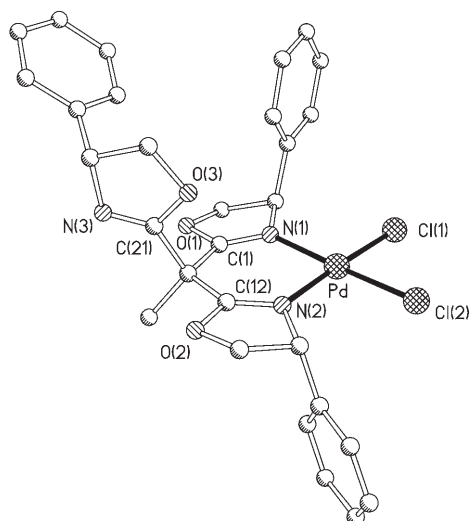


Figure 6. Molecular structure of  $[\text{PdCl}_2(\text{Ph-trisox})]$  (**1b**). Selected bond lengths ( $\text{\AA}$ ) and angles ( $^\circ$ ): Pd–N(1) 2.030(2), Pd–N(2) 2.041(2), Pd–Cl(1) 2.2915 (7), Pd–Cl(2) 2.2606(8); N(1)–C(1) 1.273(4), N(2)–C(12) 1.283(4), N(3)–C(21) 1.294(4); Cl(1)–Pd–N(1) 91.58(7), N(1)–Pd–N(2) 89.42(10), N(2)–Pd–Cl(2) 91.02(8), Cl(2)–Pd–Cl(1) 88.07(3).

zoline units (1.256(4) vs. 1.272(4) and 1.278(4)  $\text{\AA}$  for **1a** and 1.249(4) vs. 1.273(4) and 1.283(4)  $\text{\AA}$  for **1b**).

**Solution dynamics of complexes 1a–1d:** As indicated above, the  $^1\text{H}$  NMR spectrum (recorded at 400 MHz) of **1a** at 296 K is consistent with the molecular structure established for the crystalline state. Separated sets of signals, which are attributable to the protons of the three different isopropyl groups of the oxazoline units, indicate the loss of local threefold symmetry for the tripod ligand (Figure 7). The same loss of degeneracy of the three oxazoline units is observed in the  $^{13}\text{C}$  NMR spectra (75 MHz, 296 K) and the  $^{15}\text{N}$  NMR spectrum (60 MHz, 296 K). Upon increasing the temperature to 373 K coalescence occurs, and the two doublets for the  $-\text{CH}(\text{CH}_3)_2$  isopropyl protons observed in the high-temperature limiting spectrum, representing effective  $C_3$

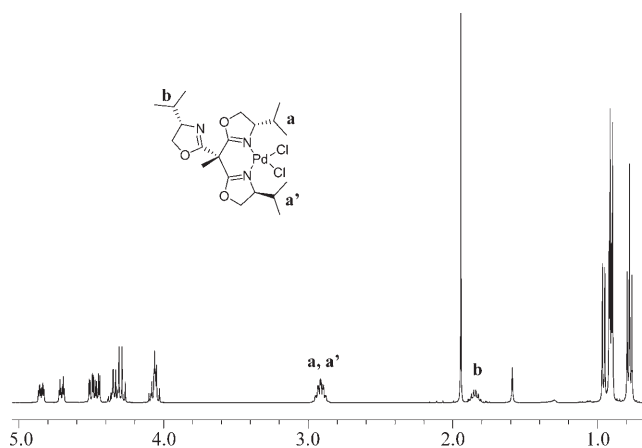


Figure 7.  $^1\text{H}$  NMR of complex  $[\text{PdCl}_2(\text{iPr-trisox})]$  (**1a**) in 1,1,2,2- $[\text{D}_2]$ tetrachloroethane at 296 K (400 MHz).

symmetry, are consistent with a fast exchange between ligating and non-ligating oxazoline rings.

To quantitatively study this exchange and to gain insight into the microscopic mechanism of this process, a systematic series of magnetisation-transfer experiments was carried out. These allowed the direct monitoring of the exchange of the protons between the coordinated oxazolines (protons **a** and **a'**,  $-\text{CHMe}_2$ ) and the non-coordinated oxazoline (proton **b**,  $-\text{CHMe}_2$ ) (Figure 7). In a series of experiments carried out with **1a** in 1,1,2,2- $[\text{D}_2]$ tetrachloroethane between 302 and 318 K, the protons of the coordinated oxazolines (**a**) were selectively inverted with a shaped pulse, followed by monitoring of the time evolution of the intensities in the two sites **a/a'** and **b**. The results of experiments in which magnetisation of protons **a** was inverted are shown in Figure 8.

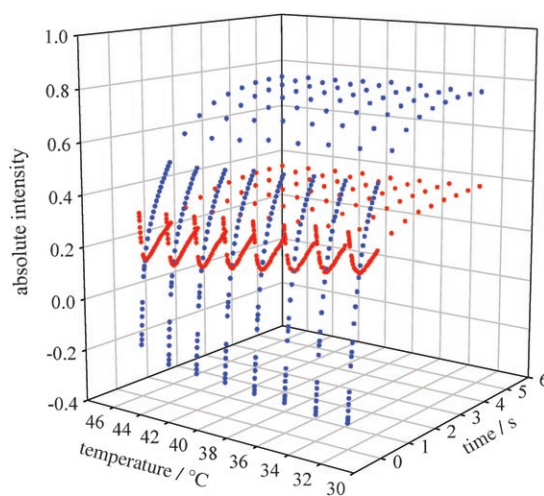


Figure 8. Time evolution of the magnetisation in the two sites (blue traces, coordinated oxazolines **a**, **a'**; red traces, non-coordinated oxazoline **b**) after selective inversion of the coordinated oxazolines resonance (complex **1a** in 1,1,2,2- $[\text{D}_2]$ tetrachloroethane). Data are shown in a pseudo-3D representation as a function of the temperature ( $^\circ\text{C}$ ).

For any given temperature  $T$ , the time dependence of the magnetisation in either of the two sites (the previously inverted site and the one connected to it by chemical exchange) could be derived directly from the McConnell equations.<sup>[18]</sup> Numerical nonlinear least-squares fits of the theoretical curves to the experimental data gave the NMR spectroscopic rate constants  $k_{\text{NMR}}(T)$  for the fluxional exchange. Taking into account the statistical factors for the fluxional exchange of the three sites,<sup>[19]</sup>  $k_{\text{NMR}}(T)$  was then converted into the chemical rate constant  $k_{\text{chem}}(T)$  (Table 1).

The Eyring plot resulting from  $k$  values obtained from inversion of the coordinated oxazoline sites is shown in Figure 9. The analysis gave an enthalpy of activation for the fluxional process of  $\Delta H^\ddagger = 75.6 \pm 0.5 \text{ kJ mol}^{-1}$  and an entropy of activation  $\Delta S^\ddagger = 14.0 \pm 1.5 \text{ J mol}^{-1}$ . Similarly, the indanyl complex **1d** (Figure 10) was studied by using the same experiment, and an enthalpy of activation for the fluxional

Table 1. Rate constants  $k_{\text{chem}}$  [ $\text{s}^{-1}$ ] for the fluxional process in complex **1a** in 1,1,2,2- $[\text{D}_2]$ tetrachloroethane (400 MHz).

$T$ [K]	Proton <b>a</b>	Proton <b>b</b>	Combined data
302	3.19	2.63	2.91
304	3.96	3.23	3.59
306	4.77	3.90	4.34
308	5.58	4.74	5.16
310	6.87	5.78	6.32
312	8.19	6.98	7.58
314	9.57	8.46	9.01
316	11.52	10.07	10.79
318	13.71	11.93	12.82

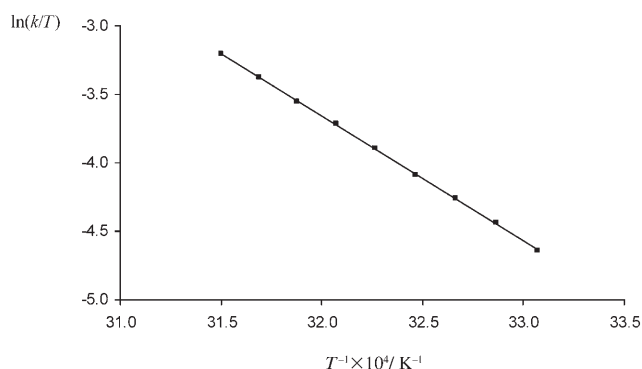


Figure 9. Eyring plot for the data from the last column of Table 1 (complex **1a**).

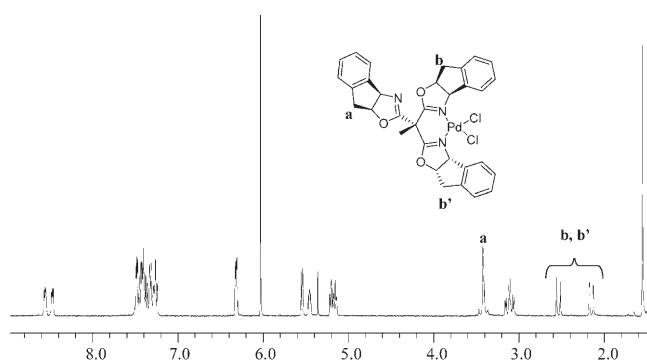


Figure 10.  $^1\text{H}$  NMR of complex  $[\text{PdCl}_2(\text{Ind-trisox})]$  (**1d**) in 1,1,2,2- $[\text{D}_2]$ tetrachloroethane at 296 K (400 MHz).

process of  $\Delta H^\ddagger = 79.4 \pm 2.0 \text{ kJ mol}^{-1}$  and an entropy of activation  $\Delta S^\ddagger = 9.3 \pm 6.0 \text{ J mol}^{-1}$  were obtained (Table 2).

Whereas the calculated enthalpy values are as expected for a dynamic process showing the qualitative behaviour described above, the small activation entropies indicate neither an associative nor a dominantly dissociative substitution mechanism. A reasonable intimate mechanism for the exchange between coordinating and non-coordinating oxazolines may resemble an interchange process. Given the ex-

Table 2. Activation parameters for the dynamic exchange of coordinated and free oxazoline rings in complexes **1a** and **1d**.

	<b>1a</b>	<b>1d</b>
$\Delta H^\ddagger$ [ $\text{kJ mol}^{-1}$ ]	$75.6 \pm 0.5$	$79.4 \pm 2.0$
$\Delta S^\ddagger$ [ $\text{J mol}^{-1}$ ]	$14.0 \pm 1.5$	$9.3 \pm 6.0$
$\Delta G^\ddagger(298 \text{ K})$ [ $\text{kJ mol}^{-1}$ ]	$71.4 \pm 0.6$	$76.4 \pm 2.8$

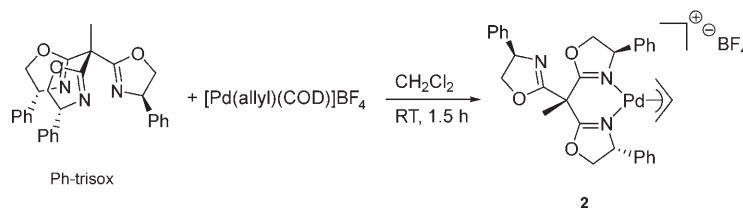
tensive body of mechanistic work carried out for substitutions at square-planar  $\text{Pd}^{\text{II}}$  complexes,<sup>[20]</sup> we assume that the interchange has slightly associative character ( $I_a$  mechanism), which implies the transient formation of a pentacoordinate palladium(II) complex in the transition state.

### Synthesis and structural characterisation of an allyl-palladium complex as a model for the key intermediate in trisox-Pd-catalysed allylic substitutions:

Since the reaction of palladium allyl derivatives with our reference tripod *i*Pr-trisox yielded oily products, we focused on the phenyl-substituted trisoxazoline derivative Ph-trisox in order to obtain a crystalline model complex for the allyl intermediates in the catalytic allylic substitution. Reaction of  $[\text{Pd}(\text{allyl})(\text{cod})]\text{BF}_4$  (cod=cyclooctadiene) with Ph-trisox in  $\text{CH}_2\text{Cl}_2$  gave the corresponding complex **2** in 52% yield (Scheme 2).

The molecular structure of complex **2** is displayed in Figure 11 and with selected bond lengths and angles given in the figure legend. The palladium atom adopts a planar coordination geometry with the  $\pi$ -allyl ligand and two of the three oxazoline rings of the trisox ligand being coordinated, and the nitrogen donors and the carbon termini of the allyl defining an approximate square. As for the dichloropalladium derivatives **1a–1d**, the third oxazoline unit is dangling with the N-donor pointing away from the palladium centre. The Pd–N and Pd–C bond lengths are within the range found for related complexes reported in the literature.<sup>[21]</sup>

The six-membered chelate ring adopts a slightly twisted boat conformation. Notably, a disorder in the central C atom of the  $\pi$ -allyl ligand is found in the crystal structure of the complex with a relative occupancy of about 2:1. This indicates a mixture of the two diastereomers in that ratio, resulting from the reduction of the  $C_2$  symmetry of the coordinated bisoxazoline due to the presence of the third uncoordinated heterocycle. The orientation of the allyl group of the major isomer is *exo* (*exo* being defined as the central C–H allylic bond pointing in the same direction as the axial methyl group).



Scheme 2. Synthesis of allyl-palladium(II) complex **2**.

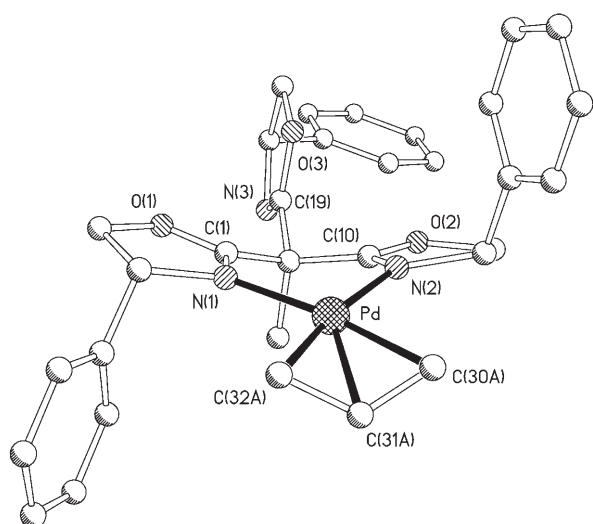


Figure 11. Molecular structure of  $[\text{Pd}(\text{Ph-trisox})(\eta^3\text{-allyl})]^+$  (**2**). For clarity, only a single orientation of the allyl ligand is shown, corresponding to the major isomer. Selected bond lengths (Å) and angles (°): Pd–N(1) 2.104(2), Pd–N(2) 2.102(2), Pd–C(32) 2.120(3), Pd–C(30) 2.131(3), N(1)–C(1) 1.279(3), N(2)–C(10) 1.274(3), N(3)–C(19) 1.264(3); C(32)–Pd–N(1) 102.16(9), N(1)–Pd–N(2) 88.14(7), N(2)–Pd–C(30) 100.85(10), C(32)–Pd–C(30) 68.87(12).

In the  $^1\text{H}$  NMR spectrum of complex **2** at room temperature, only three well-defined signals for the oxazoline protons are observed indicating fast exchange between the three heterocycles as well as between the *exo* and *endo* diastereomers. Five signals are observed for the allyl moiety as expected for a dissymmetrical  $\pi$ -allyl ligand (Figure 12), the

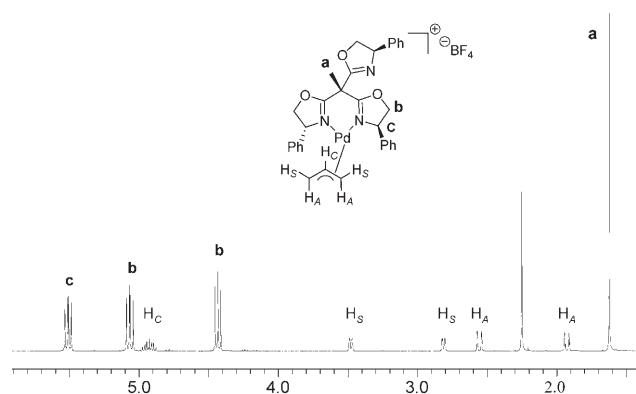


Figure 12.  $^1\text{H}$  NMR of complex  $[\text{Pd}(\text{Ph-trisox})(\eta^3\text{-allyl})]\text{BF}_4$  (**2**) in  $\text{CDCl}_3$  at 296 K (400 MHz).

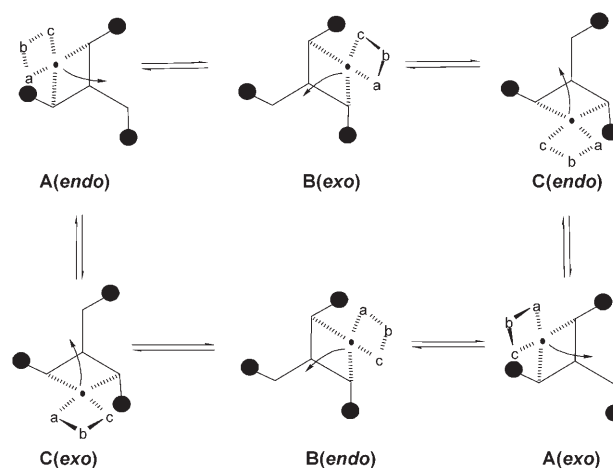
partial assignment being based on a  $^1\text{H}$  NOESY experiment. In addition to the negative phase non-diagonal NOE cross-peaks, EXSY signals between *syn* and *anti* protons were observed, indicating slow exchange between  $\eta^3$ -allyl and  $\eta^1$ -allyl forms.

A series of variable-temperature (VT)  $^1\text{H}$  NMR experiments performed in the range of 296 to 373 K indicated no spectral changes for the allyl proton resonances, neither be-

tween the pairs of the *syn* or *anti* protons nor cross exchange among them. As previously observed for other non-symmetrical allyl complexes, this is consistent with the stereochemical rigidity of the allyl–Pd fragment on the timescale of the experiments; in other words, it is not affected by the interchange of the oxazoline coordination as well as the (possibly concomitant) interconversion of *exo* and *endo* diastereomers.<sup>[22]</sup>

To quantify the latter, a low-temperature  $^1\text{H}$  NMR study was carried out. Coalescence of the trisoxazoline ligand resonances occurred at 198 K; however, the low-temperature-limit was not attained at 190 K (in  $\text{CD}_2\text{Cl}_2$ ). Although the exchange of the three oxazolines was not completely frozen, an estimate of the activation barrier  $\Delta G^\ddagger$  for the oxazoline exchange of ca.  $55 \text{ kJ mol}^{-1}$  may be derived. At low temperature, the resonance pattern of the ligand is thus consistent with the bidentate N,N-chelation observed in the solid state. Notably, the signals of the allyl fragment begin to broaden at 190 K, presumably owing to the slowing down of the *exo/endo* exchange; however, complete decoalescence was not obtained.

The stereochemical rigidity of the allyl–Pd fragment on the VT-NMR timescale and the observation that the oxazoline exchange and the *exo/endo* isomerisation are associated with similarly low activation barriers may indicate that the last two are mechanistically coupled; that is, that the trisox “walk-about” and the reorientation of the allyl–Pd unit occur by the same route. A possible pathway, based on a stereospecific interchange of the oxazolines is proposed in Scheme 3, which extends the proposed general exchange pathway of Figure 3.



Scheme 3. Possible exchange pathway, based on a stereospecific interchange of the oxazolines which extends the proposed general exchange pathway of Figure 3.

**Synthesis, structural characterisation and dynamic behaviour of trisox-palladium(0) complexes:** Having explored the coordination chemistry with palladium(II), we then turned our attention to zero-valent palladium complexes, which represent the other intermediates in the catalytic cycle of allylic

substitutions. Compared to the extensive work on phosphane- $\eta^2$ -alkene palladium(0) complexes, there are only few well defined  $[\text{Pd}(0)(\eta^2\text{-alkene})]$  complexes that contain ancillary nitrogen-donor ligands.<sup>[23]</sup> In particular, we note that there is no report of structurally characterised  $\text{Pd}^0$  complexes containing oxazoline-based ligands. Palladium(0) compounds are generally either formed in situ by reduction of a suitable palladium(II) precursor, or by starting from a zero-valent palladium precursor complex containing labile ligands. Attempts to reduce the  $[\text{PdCl}_2(\text{trisox})]$  complexes described in the previous sections did not lead to the expected palladium(0) complexes; however, an alternative synthetic route starting from zero-valent palladium complexes was successful.

A number of palladium(0) complexes with different ligands (including a potentially tridentate pyridine-bisoxazoline ligand (vide infra) and alkenes were synthesised (Scheme 4) by using complexes of general formula  $[\text{Pd}(\text{nbd})(\text{alkene})]$  (nbd = norbornadiene; alkene = maleic anhydride or tetracyanoethylene) as precursor.<sup>[23a,24]</sup> Complexes **3a–e** were obtained by substitution of the nbd ligand by the respective tripod ligand in THF and were isolated as highly air sensitive yellow powders in 50–75% yield.

The molecular structure of compound **3a** is presented in Figure 13 along with the principal geometric parameters. For palladium(0) complexes, both a trigonal planar or a tetrahedral molecular geometry would be expected in case of a facial tridentate ligand. Complex **3a** possesses Y-shaped trigonal-planar geometry with the trisox ligand coordinated in a bidentate fashion, whilst the third oxazoline unit is dan-

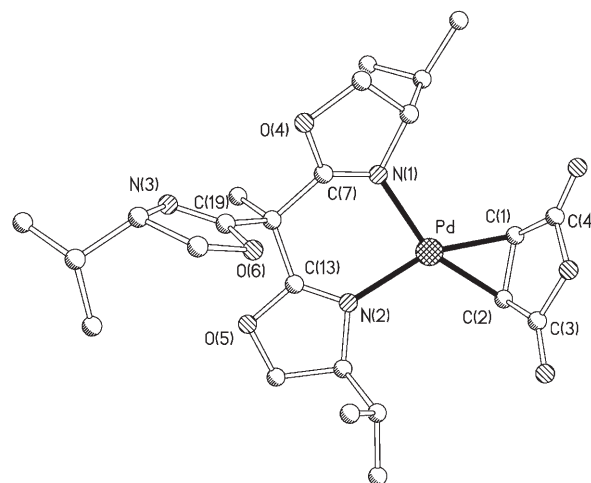
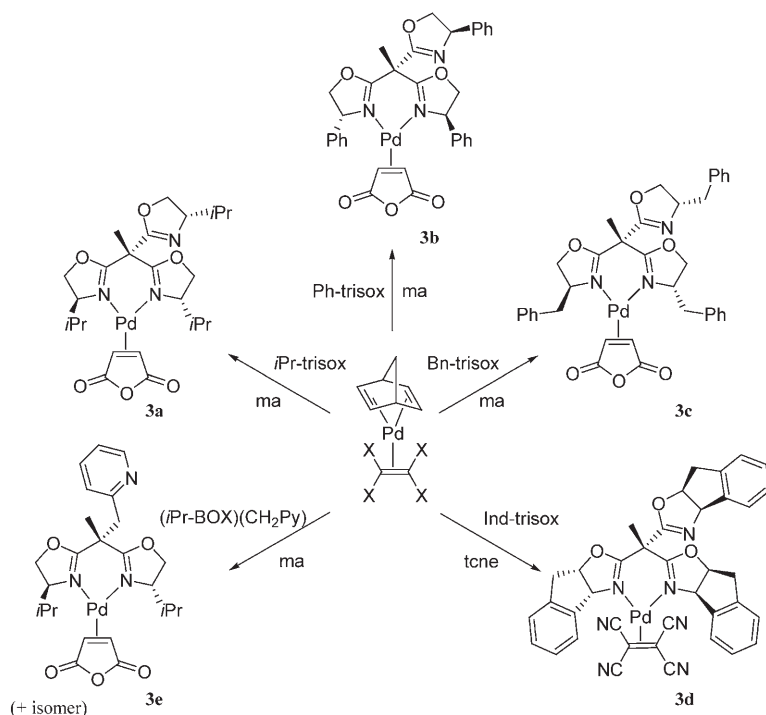


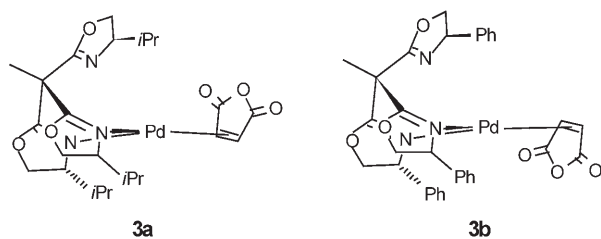
Figure 13. Molecular structure of  $[\text{Pd}(i\text{Pr-trisox})(\text{ma})]$  (**3a**). Selected bond lengths (Å) and angles (°): Pd–N(1) 2.127(5), Pd–N(2) 2.115(4), Pd–C(1) 2.107(7), Pd–C(2) 2.082(6), N(1)–C(7) 1.261(7), N(2)–C(13) 1.261(7), N(3)–C(19) 1.254(9), C(1)–C(2) 1.448(9); N(1)–Pd–N(2) 85.6(2), N(2)–Pd–C(2) 116.9(2), C(1)–Pd–N(1) 117.6(2), C(1)–Pd–C(2) 40.4(2); torsion angle C(3)–C(2)–C(1)–Pd  $-98.4^\circ$ .

gling with the N-donor pointing away from the metal centre. The Pd–N (2.127(5) Å) and Pd–C (2.082(6) Å) bond lengths are in agreement with reported values for similar complexes that contain bidentate nitrogen-based ligands such as *t*BuDAB (*t*BuDAB = di-*tert*-butyl-1,4-diazabutadiene).<sup>[25]</sup> The N(1)–Pd–N(2) angle of 85.6(2)° is greater than those reported for related complexes (typically 77.2–77.5°).<sup>[26]</sup> This increase in bite angle is due to the six-membered chelate ring of a bidentate trisoxazoline with respect to the values of five-membered rings described in the literature. As expected, upon coordination of the alkene an elongation of the C=C bond distance (1.448(9) Å) with respect to the free alkene (1.3322(9) Å) is observed.<sup>[27]</sup> It is of interest to note that although an equilibrium of two diastereomers is observed in solution at ambient temperature, the crystals employed for the X-ray diffraction study of **3a** consisted only of one diastereomeric form.

In the crystals of the phenyl-substituted complex **3b**, the other of the two diastereomers is exclusively found. Apart from that, the gross molecular structure appears similar to that of **3a**. However, the quality of the data was only suffi-



Scheme 4. Palladium(0) complexes **3a–e** (nbd = norbornadiene, ma = maleic anhydride, tene = tetracyanoethylene).



cient to unequivocally establish the molecular connectivity and configuration, but did not allow a more detailed appreciation of the structure.

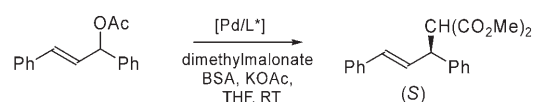
$^1\text{H}$  NMR spectra of all complexes recorded at 296 K represent a dynamic exchange regime for the trisox ligand as well as the equilibrium between the diastereomers due to the different orientation of the  $\pi$ -bonded maleic anhydride ligand relative to the pendant oxazoline arm. Upon lowering the temperature, these fluxional processes are frozen for complexes **3a–c** and two sets of resonances attributable to the two diastereomers are observed. For complex **3b** the ratio was found to be 1:1.1 and the measured activation barrier  $\Delta G^\ddagger(261\text{ K}) = 55\text{ kJ mol}^{-1}$ . The isomer interconversion may, in principle, be caused by either an olefin rotation or a decoordination–coordination process that involves the alkene and/or the ligand. The  $\Delta G^\ddagger$  values reported in the literature for alkene rotation are usually around 60–70  $\text{kJ mol}^{-1}$ ,<sup>[28]</sup> however, energy barriers of 50  $\text{kJ mol}^{-1}$  have also been noted.<sup>[29]</sup> In the case of complex **3b**, it is therefore difficult to conclude on the exact mechanism, since the ligand may be involved in the process.

In the case of complex **3d**, which contains tetracyanoethylene as  $\pi$ -bonded alkene, the resonance pattern of the oxazoline protons is consistent with effective  $C_3$  symmetry and thus rapid exchange between the three heterocycles. Lowering the temperature leads to coalescence at 243 K and the non-symmetrical low-temperature limiting spectrum at 198 K. A simulation of the dynamic NMR spectra gave an activation barrier of  $\Delta G^\ddagger(298\text{ K}) = 42 \pm 5\text{ kJ mol}^{-1}$ .

Whereas the trisox–Pd complexes **3a–3d** contain three-fold symmetrical tripods, complex **3e** contains a bisoxazoline ligand to which a 2-pyridylmethyl sidearm has been added. This renders the ligand completely non-symmetrical and thus—as indicated in Figure 2 for  $C_1$  symmetric tripods—there are potentially three species, which differ in the way the ligand is coordinated to the metal centre. Apart from an isomer with two oxazoline units bound to the metal there are two closely related but diastereomeric forms with one oxazoline ring and the pyridine arm bound to the metal. Whereas the  $^1\text{H}$  NMR spectra recorded at 296 K represent an intermediate dynamic regime, the exchange between the different diastereomers was frozen out at 218 K. Notably, a 1:1 equilibrium mixture of the bisoxazoline complex on the one hand and the two forms of the oxazolin–pyridine isomer on the other are observed. Since the oxazolin–pyridine isomers possess near-identical overlapping resonance patterns they were treated as one species in the analysis of the dynamic process. The situation is complicated by the fact that

the  $\pi$ -coordinated maleic anhydride may adopt two possible orientations with respect to the pendant arm, which is either an oxazoline or the  $\text{CH}_2\text{Py}$  arm. By means of a VT  $^1\text{H}$  NMR study the high-temperature limit for these exchange processes between a total of six diastereomers was attained and an effective free enthalpy of activation for the overall process of bisoxazoline/oxazolin–pyridine exchange of  $\Delta G^\ddagger(315\text{ K}) \approx 63\text{ kJ mol}^{-1}$  was estimated.

**Palladium-catalysed asymmetric allylic alkylation with trisoxazolines and related stereodirecting ligands:** As a test reaction that is mechanistically very well understood and may thus serve as a probe for studying the catalytic behaviour of the new Pd complexes, the allylic alkylation of 1,3-diphenylprop-2-enyl acetate substrate with dimethyl malonate as nucleophile (in the presence of *N,O*-bis(trimethylsilyl)acetamide (BSA)) was chosen. The reaction was carried out by using the catalytic systems prepared in situ by addition of the ligand to the palladium allyl chloride  $[\text{PdCl}(\eta^3\text{-C}_3\text{H}_5)]_2$  precursor (Scheme 5).<sup>[30]</sup>



Scheme 5. Palladium-catalysed allylic alkylation of 1,3-diphenylprop-2-enyl acetate.

Pfaltz and co-workers previously investigated this reaction with the well-established bisoxazoline (BOX) ligands as stereodirecting ligands, and this particular system therefore provided the point of reference for the catalytic study at hand. By using 2.2 mol % of palladium and the *iPr*-BOX ligand, an enantiomeric excess (*ee*) of 89 % and 89 % isolated yield were obtained after three days in good agreement with Pfaltz's results (Table 3, entry 1).<sup>[31]</sup> Under the same conditions, the analogous catalyst with *iPr*-trisox as stereodirecting ligand gave an *ee* of 95 % and 90 % yield. As a similar comparative study with the other oxazoline derivatives showed, the trisoxazoline-based catalysts generally induce a better enantioselectivity compared to their bisoxazoline ana-

Table 3. Results of asymmetric allylic alkylation with various bisoxazolines and trisoxazolines.<sup>[a]</sup>

Entry	R	Ligand		Ligand	
		Yield [%]	<i>ee</i> [%]	Yield [%]	<i>ee</i> [%]
1	( <i>S</i> )- <i>iPr</i>	89	89	90	95
2	( <i>R</i> )-Ph	7	–72	28	–88
3	( <i>S</i> )-Bn	88	83	92	88
4	(4 <i>R</i> ,5 <i>S</i> )-Ind	13	–93	95	–98

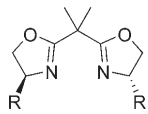
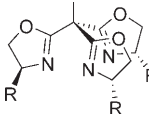
[a] Experimental conditions: catalytic precursor generated in situ from  $[\text{PdCl}(\eta^3\text{-C}_3\text{H}_5)]_2$  and ligand (1.1 mol %, ratio ligand/Pd = 1.1) in THF at 50 °C for 1.5 h; catalysis carried out at room temperature; yields and *ee* determined after 72 h.



logues, and this behaviour appears to be independent of the substituent as shown on Table 3.

In a further comparative study, the catalytic conversions with the BOX and trisox ligands from Table 3 were monitored by gas chromatography (Figure 14). The most notable observation is the rate acceleration with the tripods compared to the BOX ligands for all substitution patterns. The turn-over frequencies (TOFs) derived from the quasilinear section in the conversion curves are displayed in Table 4.

Table 4. Turn-over frequencies TOF [ $\text{h}^{-1}$ ] derived from the conversion curves shown in Figure 14.

R			TOF ratio Trisox/BOX
( <i>S</i> )- <i>i</i> Pr	1.37	5.02	3.7
( <i>R</i> )-Ph	0.05	0.2	4
( <i>S</i> )-Bn	0.91	3.73	4.1
(4 <i>R</i> ,5 <i>S</i> )-Ind	0.19	12.2	64.2

The rate of the reaction is strongly dependent on the substituent of the respective ligand, with the *i*Pr substituent yielding the most active BOX-derivative, whereas the indanyl substituent leads to the highest rate for the trisox-based catalysts. With *i*Pr, Ph and Bn-based ligands, the TOFs differ by a factor of four in favour of the tripod, whilst a striking 64-fold acceleration was found for the indanyl-derivative!

To explore the role of the third oxazoline unit, a series of modified bisoxazoline ligands containing potentially coordinating or non-coordinating "sidearms" at the apical position

were synthesised by reaction of the monolithiated 1,1-bis-(oxazoliny)ethane with the appropriate electrophiles. Additionally, we also synthesised several dually functionalised  $\text{C}_2$  symmetric systems that are readily obtained from the bis-(oxazoliny)methane.

The results of the asymmetric allylic alkylations are summarised in Table 5 (together with previously discussed *i*Pr-BOX/*i*Pr-trisox couple, entries 1–2). In general, the highest yields were obtained from ligands that contain a potentially donating heteroatom as sidearm, with ligands that contain nitrogen donors displaying slightly higher activity than oxygen donors. The enantioselectivity of the product is also affected by the nature of the sidearm. For example, methylpyridyl as sidearm gave moderate to very low enantioselectivity (entries 6 and 10), whilst the introduction of ketone units appear to give more selective catalysts (entries 4 and 5). Ligands with no heteroatom-containing sidearms usually give lower yields (entries 1,7–9) and moderate to good enantiomeric excesses, depending on the bulkiness of the substituents.

A comparative study of the catalytic conversion with two representative non-symmetric side-arm-functionalised ligands ( $-\text{CO}t\text{Bu}$ , entry 4 and  $-\text{CH}_2\text{Py}$ , entry 6) was carried out and compared with the results obtained for *i*Pr-BOX and *i*Pr-trisox systems (Figure 15). Whereas the introduction of a donating sidearm leads to rate enhancement, none of the catalysts containing the non-symmetrical stereodirecting ligands reach the activity obtained with the trisoxazoline ligand *i*Pr-trisox.

The mechanism of palladium-catalysed allylic alkylation is generally thought to involve four steps.<sup>[12,13]</sup> After coordination of the substrate to the palladium(0) species, an oxidative addition results in the formation of the  $\pi$ -allyl palladi-

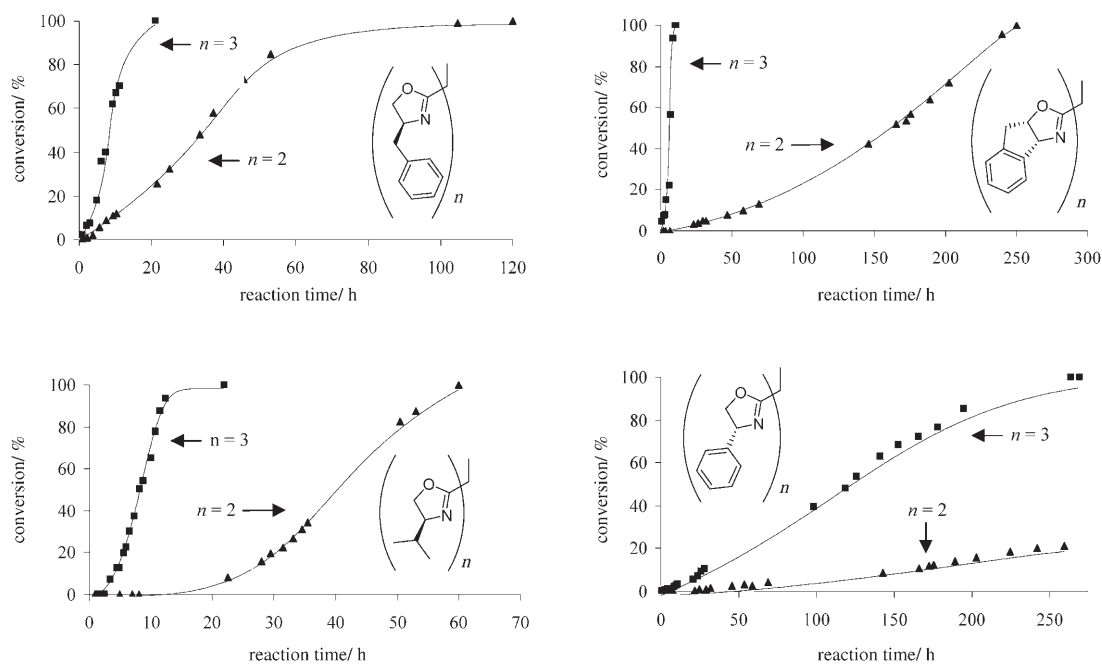


Figure 14. Comparison of the conversion curves for the Pd/trisoxazoline systems (■) and the corresponding Pd/bisoxazoline systems (▲).

Table 5. Results of asymmetric allylic alkylation of 1,3-diphenylprop-2-enyl acetate with dimethylmalonate.<sup>[a]</sup>

Entry	Ligand	Yield [%]	ee [%]
1		89	89
2		90	95
3		67	91
4		74	95
5		68	95
6		93	66
7		15	86
8		51	94
9		63	93
10		84	3

[a] Experimental conditions: catalyst precursor generated in situ by stirring  $[(\text{PdCl}(\eta^3\text{-C}_3\text{H}_5)_2)_2]$  and ligand (1.1 mol%, ratio ligand/Pd=1.1) in THF at 50°C for 1.5 h; catalysis carried out at ambient temperature; yields and ee determined after a reaction time of 72 h.

um(II) complex. The nucleophile then externally attacks the  $\pi$ -allyl intermediate giving rise to a palladium(0) species at

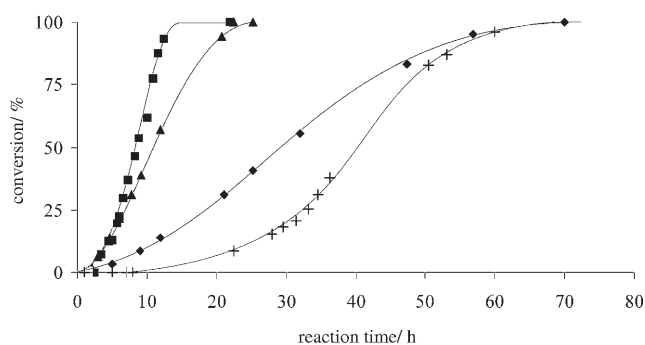


Figure 15. Comparison of the conversion curves for the following catalyst systems: Pd/(iPr-trisox) (■), Pd/[(iPr-BOX)CH<sub>2</sub>Py] (▲), Pd/(iPr-BOX) (+) and Pd/[(iPr-BOX)COtBu] (◆) (see entries 2, 6, 1 and 4 in Table 5, respectively).

which the product may be displaced by way of substitution through another substrate molecule.

Since our catalytic systems were prepared in situ from palladium(II) allyl chloride and the trisox ligand, the first step in the formation of the active catalyst involves the reduction of the palladium(II) precursor by a nucleophilic attack by the carbanionic species. The observation of an induction period in the conversion curves is thus not surprising. Introduction of an additional donor function in the stereodirecting ligand generally resulted not only in a rate enhancement, but also the reduction of this induction period. The observed overall rate acceleration might be due to the ability of the additional donating group to induce the formation of the palladium(0) species both in the initial generation of the active species as well as in the product/substrate exchange step at the end of the catalytic cycle.

This mechanistic aspect, as well as the symmetry-related simplification of the reaction network for the catalysts bearing C<sub>3</sub>-chiral tripods, may be at the root of the superior performance of the trisox systems.

## Conclusion

In this work we have demonstrated the potential of C<sub>3</sub>-chiral trisox ligands in enantioselective catalytic transformation in which the complex intermediate in the selectivity-determining step does not adopt a deltahedral coordination geometry and thus does not allow tripodal coordination of the stereodirecting ligand. Instead, the presence of the additional donor function appears to play a role in the subsequent product/substrate exchange step as well as in the initial generation of the active catalyst. Since the key intermediate contains a dicoordinate tripod with a dangling ligand arm, with dynamic exchange between the donor functions, the use of a C<sub>3</sub>-symmetric trisoxazoline significantly reduces the number of interconverting isomers. This simplification of the catalytic reaction network appears to be manifested in superior catalyst performance for such species. Notably, the system with the least internal degrees of free-

dom, the catalyst bearing the indanyl-trisox ligand displays the highest activity and selectivity.<sup>[32]</sup>

## Experimental Section

All manipulations, except those indicated otherwise, were carried out under an inert atmosphere of dry argon using standard Schlenk techniques. Solvents were purified and dried by standard methods. The starting materials (*R*)-phenylglycinol,<sup>[33]</sup> (*S*)-phenylalaninol,<sup>[33]</sup> 1,1-bis[(4*R*)-4-phenyl-1,3-oxazolin-2-yl]ethane,<sup>[34]</sup> (4*R*)-4-phenyloxazoline,<sup>[35]</sup> (4*S*)-4-benzyloxazoline,<sup>[35]</sup> bis[(4*R,S*)-4,5-indanediylloxazolin-2-yl]methane,<sup>[36]</sup> [Pd(cod)(η<sup>3</sup>-C<sub>3</sub>H<sub>5</sub>)<sub>2</sub>BF<sub>4</sub>]<sup>[37]</sup> [Pd(η<sup>2</sup>,η<sup>2</sup>-nbd)(η<sup>2</sup>-ma)]<sup>[23a]</sup> [Pd(η<sup>2</sup>,η<sup>2</sup>-nbd)(η<sup>2</sup>-tnc)]<sup>[23a]</sup> 2,2-bis[(4*S*)-4-isopropylloxazolin-2-yl]-1-(pyridin-2-yl)popane,<sup>[15a]</sup> 2,2-bis[(4*S*)-4-isopropylloxazolin-2-yl]-1-phenylpropane,<sup>[15a]</sup> and 2,2-bis[(4*S*)-4-isopropylloxazolin-2-yl]-1,3-diphenylpropane,<sup>[38]</sup> as well as (4*S*)-2-bromo-4-benzyloxazoline,<sup>[39]</sup> (4*R,S*)-2-bromo-4,5-indanediylloxazoline,<sup>[39]</sup> (4*R*)-2-bromo-4-phenyloxazoline<sup>[39]</sup> were synthesised according to literature procedures. 2,2-Bis[(4*S*)-4-isopropylloxazolin-2-yl]-4,4-dimethylpentan-3-one, 2,2-bis[(4*S*)-4-isopropylloxazolin-2-yl]-1-phenylpropan-1-one, 2,2-bis[(4*S*)-4-isopropylloxazolin-2-yl]-1,3-di(naphth-2-yl)propane and 2,2-bis[(4*S*)-4-isopropylloxazolin-2-yl]-1,3-di(pyrin-2-yl)propane were obtained according to previously published protocols.<sup>[40]</sup> All other reagents were commercially available and were used without further purification. <sup>1</sup>H and <sup>13</sup>C NMR spectra were recorded on a Bruker DRX 200 spectrometer at 200 MHz and 50 MHz, respectively, on a Bruker Avance 300 spectrometer at 300 MHz and 75 MHz, respectively, on a Bruker Avance II 400 spectrometer at 400 MHz and 100 MHz, respectively, and on a Bruker Avance III 600 spectrometer at 600 MHz and 150 MHz, respectively, and were referenced using the residual proton or <sup>13</sup>C solvent peak. <sup>15</sup>N NMR spectra were recorded on a Bruker Avance III 600 spectrometer equipped with a cryogenically cooled direct detection probe (QNP-cryoprobe™, optimised for detection of <sup>31</sup>P, <sup>13</sup>C and <sup>15</sup>N). The experimental parameters for the direct <sup>15</sup>N detection were optimised with a 0.2 M solution of a non-enriched N-ligand titanium complex. For routine direct <sup>15</sup>N NMR detection concentrations of not less than 0.1 M are necessary. Selected parameters are: Puls-program: inverse gated decoupled; relaxation delay 6 s; 90°-<sup>15</sup>N-puls (10 μs); pre-acquisition delay 400 μs; time domain 64 K; sweep 500 ppm; acquisition time 1 s; number of accumulations 5000. Processing: 60 points of backward linear prediction in order to minimise base-line artefacts; exponential window function with 0.3 Hz line broadening factor. Infrared spectra were obtained on a Perkin-Elmer 1600 FT-IR spectrometer. Mass spectra and elemental analysis were recorded by the analytical services of the Strasbourg and Heidelberg chemistry departments.

### Preparation of the trisox ligands and their precursors

**1,1,1-Tris[(4*R*)-4-phenyloxazolin-2-yl]ethane:** *t*BuLi (1.2 mL, 1.7 M in pentane, 2 mmol) was added dropwise to a solution of 1,1-bis[(4*R*)-4-phenyloxazolin-2-yl]ethane (535 mg, 1.8 mmol)<sup>[34]</sup> in THF (60 mL) at -78°C. The resulting yellow solution was stirred for an additional 30 min prior to the addition of (4*R*)-2-bromo-4-phenyloxazoline (1.2 equiv, 453 mg, 2 mmol).<sup>[39]</sup> The solution was allowed to warm slowly to room temperature over 12 h and then concentrated to remove the pentane and finally the Schlenk tube was sealed. The stirred solution was heated at 70°C for 5 d. The resulting orange solution was evaporated to dryness. The residue was redissolved in dichloromethane (100 mL) and washed with water (10 mL). The organic extract was dried over Na<sub>2</sub>SO<sub>4</sub> and concentrated in vacuo to give a yellow solid. Purification by crystallisation from CH<sub>2</sub>Cl<sub>2</sub>/pentane gave the desired product (470 mg, 60% yield). <sup>1</sup>H NMR (200 MHz, CDCl<sub>3</sub>, 296 K): δ = 2.06 (s, 3H; CH<sub>3</sub>), 4.27 (dd, *J* = 7.8, 8.3 Hz, 3H; CH<sub>2</sub>oxa), 4.76 (dd, *J* = 8.3, 10.1 Hz, 3H; CH<sub>2</sub>oxa), 5.32 (dd, *J* = 7.7, 10.1 Hz, 3H; CH<sub>oxa</sub>), 7.30 ppm (m, 15H; CH<sub>arom</sub>); <sup>13</sup>C {<sup>1</sup>H} NMR (50 MHz, CDCl<sub>3</sub>, 296 K): δ = 21.4 (CH<sub>3</sub>), 45.2 ((CH<sub>3</sub>)C(oxa)<sub>3</sub>), 69.7 (CH<sub>oxa</sub>), 76.0 (CH<sub>2</sub>oxa), 126.9, 127.6, 128.7 (C<sub>arom</sub>), 142.1 (C<sub>quat-arom</sub>), 166.1 ppm (NCO); FT-IR (KBr):  $\tilde{\nu}$  = 1665 cm<sup>-1</sup> (s, C=N); MS (EI): *m/z* (%): 465.7 (92) [M<sup>+</sup>]; elemental analysis calcd (%) for C<sub>29</sub>H<sub>27</sub>N<sub>3</sub>O<sub>3</sub>: C 74.82, H 5.85, N 9.03; found: C 74.70, H 5.81, N 8.99.

**1,1-Bis[(4*R,S*)-4,5-indanediylloxazolin-2-yl]ethane:** A solution of LDA (0.9 mL, 2 M in THF/pentane, 1.8 mmol) was added dropwise to a solution of bis[(4*R,S*)-4,5-indanediylloxazolin-2-yl]methane (552 mg, 1.7 mmol)<sup>[36]</sup> in THF (25 mL) at -78°C. The brown solution of the anion was allowed to warm to ambient temperature and stirred for an additional 0.5 h prior to the addition of methyl trifluoromethanesulfonate (0.20 mL, 1.8 mmol). The colourless solution was stirred for 12 h and was concentrated to dryness. The residue was redissolved in dichloromethane (60 mL) and washed with a saturated aqueous solution of NH<sub>4</sub>Cl (10 mL) and brine (10 mL). The organic extract was dried over Na<sub>2</sub>SO<sub>4</sub> and concentrated in vacuo to give a yellowish solid. Purification by flash chromatography (hexane/EtOAc, 50:50) gave the desired product as a white solid (340 mg, 59% yield). <sup>1</sup>H NMR (400 MHz, CD<sub>2</sub>Cl<sub>2</sub>, 296 K): δ = 1.35 (d, *J* = 7.2 Hz, 3H; CH<sub>3</sub>), 3.03 (m, 2H; CH<sub>2</sub>Ind), 3.39 (m, 3H; CH<sub>2</sub>Ind, CH<sub>bridge</sub>), 5.30 (m, 2H; OCH<sub>oxa</sub>), 5.52 (d, *J* = 8.0 Hz, 2H; NCH<sub>oxa</sub>), 7.28 (m, 6H; CH<sub>arom</sub>), 7.45 ppm (m, 2H; CH<sub>arom</sub>); <sup>13</sup>C {<sup>1</sup>H} NMR (100 MHz, CD<sub>2</sub>Cl<sub>2</sub>, 296 K): δ = 14.6 (CH<sub>3</sub>), 33.9 (CH<sub>bridge</sub>), 39.7 (CH<sub>2</sub>Ind), 76.6 (NCH<sub>oxa</sub>), 83.2 (OCH<sub>oxa</sub>), 125.3, 127.2, 128.3 (C<sub>arom</sub>), 139.9, 141.9 (C<sub>quat-arom</sub>), 165.6 ppm (NCO); FT-IR (KBr):  $\tilde{\nu}$  = 1653 cm<sup>-1</sup> (s, C=N); MS (EI): *m/z* (%): 344.4 (81) [M<sup>+</sup>]; elemental analysis calcd (%) for C<sub>22</sub>H<sub>20</sub>N<sub>2</sub>O<sub>2</sub>: C 76.72, H 5.85, N 8.13; found: C 76.61, H 5.89, N 8.17.

**1,1,1-Tris[(4*R,S*)-4,5-indanediylloxazolin-2-yl]ethane:** *t*BuLi (0.52 mL, 1.5 M in pentane, 0.77 mmol) was added dropwise to a solution of 1,1-bis[(4*R,S*)-4,5-indanediylloxazolin-2-yl]ethane (222 mg, 0.64 mmol) in toluene (60 mL) at -85°C. The resulting yellow solution was stirred for an additional 30 min prior to the addition of a solution of (4*R,S*)-2-bromo-4,5-indanediylloxazoline (346 mg, 1.45 mmol)<sup>[39]</sup> in cold toluene (4 mL). The solution was allowed to warm slowly to room temperature for 12 h and then concentrated to remove the pentane and finally the Schlenk tube was sealed. The stirred solution was heated at 60°C for two days. The resulting orange solution was evaporated to dryness. The residue was redissolved in dichloromethane (100 mL) and washed with a saturated aqueous solution of NaHCO<sub>3</sub> (10 mL) and brine (10 mL). The organic extract was dried over Na<sub>2</sub>SO<sub>4</sub> and concentrated in vacuo to give an orange foam. Purification by flash chromatography (hexane/EtOAc, 80:20) gave the desired product as a yellowish solid (100 mg, 31% yield). <sup>1</sup>H NMR (400 MHz, CD<sub>2</sub>Cl<sub>2</sub>, 296 K): δ = 1.60 (s, 3H; CH<sub>3</sub>), 3.04 (dd, *J* = 1.8, 18.0 Hz, 3H; CH<sub>2</sub>Ind), 3.33 (dd, *J* = 7.2, 18.1 Hz, 3H; CH<sub>2</sub>Ind), 5.29 (ddd, *J* = 2.1, 7.2, 8.0 Hz, 3H; OCH<sub>oxa</sub>), 5.49 (d, *J* = 8.0 Hz, 3H; NCH<sub>oxa</sub>) 7.25 (m, 9H; CH<sub>arom</sub>), 7.36 ppm (d, *J* = 7.2 Hz, 3H; CH<sub>arom</sub>); <sup>13</sup>C {<sup>1</sup>H} NMR (100 MHz, CD<sub>2</sub>Cl<sub>2</sub>, 296 K): δ = 21.3 (CH<sub>3</sub>), 22.4 ((CH<sub>3</sub>)C(oxa)<sub>3</sub>), 39.9 (CH<sub>2</sub>Ind), 76.9 (NCH<sub>oxa</sub>), 84.0 (OCH<sub>oxa</sub>), 125.5, 125.8, 127.5, 128.7 (C<sub>arom</sub>), 140.4, 141.9 (C<sub>quat-arom</sub>), 164.7 ppm (NCO); FT-IR (KBr):  $\tilde{\nu}$  = 1653 cm<sup>-1</sup> (s, C=N); MS (FAB): *m/z* (%): 502.4 (100) [M<sup>+</sup>]; elemental analysis calcd (%) for C<sub>32</sub>H<sub>27</sub>N<sub>3</sub>O<sub>3</sub>: C 76.63, H 5.43, N 8.38; found: C 76.50, H 5.47, N 8.45.

**1,1-Bis[(4*S*)-4-benzyloxazolin-2-yl]ethane:** Diethylmethylmalonate (2.8 mL, 16.3 mmol) and (*S*)-phenylalaninol were added in a Schlenk flask. NaH (10 mg, 0.25 mmol; 60% dispersion in mineral oil) was then added under nitrogen to the flask which was sealed and heated to 130°C. After 16 h, the ethanol was removed under vacuum to leave a white solid pure enough to be used for the next step without further purification (5.9 g, 95%). A solution of TsCl (5.9 g, 30.8 mmol) in CH<sub>2</sub>Cl<sub>2</sub> (30 mL) was slowly added to an ice-cooled solution of the dihydroxy diamide prepared in the previous step (5.9 g, 15.4 mmol), triethylamine (17.2 mL, 123.2 mmol) and DMAP (188 mg, 1.54 mmol) in CH<sub>2</sub>Cl<sub>2</sub> (200 mL). The mixture was warmed to room temperature, was stirred for 3 d and was washed with a saturated aqueous solution of NH<sub>4</sub>Cl and brine. The organic phase was dried over Na<sub>2</sub>SO<sub>4</sub> and was concentrated in vacuo to give a yellow oil. Purification by flash chromatography (CH<sub>2</sub>Cl<sub>2</sub>/MeOH/Et<sub>3</sub>N, 97:3:1) gave the desired product as a colourless oil (2.4 g, 45% yield). <sup>1</sup>H NMR (200 MHz, CDCl<sub>3</sub>, 296 K) δ = 1.46 (d, *J* = 7.2 Hz, 3H; CH<sub>3</sub>), 2.67 (dd, *J* = 8.5, 13.7 Hz, 2H; CH<sub>2</sub>Bn), 3.11 (dd, *J* = 5.0, 13.7 Hz, 2H; CH<sub>2</sub>Bn), 3.48 (q, *J* = 7.2 Hz, 1H; CH<sub>bridge</sub>), 4.00 (dd, *J* = 7.4, 8.3 Hz, 2H; CH<sub>2</sub>oxa), 4.20 (m, 2H; CH<sub>2</sub>oxa), 4.42 (m, 2H; CH<sub>oxa</sub>), 7.23 ppm (m, 10H; CH<sub>arom</sub>); <sup>13</sup>C {<sup>1</sup>H} NMR (50 MHz, CDCl<sub>3</sub>, 296 K): δ = 15.2 (CH<sub>3</sub>), 33.9 (CH<sub>bridge</sub>), 41.4 (CH<sub>2</sub>Bn), 67.2 (CH<sub>oxa</sub>), 72.1 (CH<sub>2</sub>oxa), 126.5, 128.5, 129.3 (C<sub>arom</sub>), 137.7 (C<sub>quat-arom</sub>), 166.1 ppm (NCO); FT-IR (KBr):  $\tilde{\nu}$  = 1661 cm<sup>-1</sup> (s, C=N); MS (EI): *m/z* (%): 257.1 (100) [M<sup>+</sup>-CH<sub>2</sub>Ph] 348.2

(50) [ $M^+$ ]; elemental analysis calcd (%) for  $C_{22}H_{24}N_2O_2$ : C 75.83, H 6.94, N 8.04; found: C 75.62, H 6.99, N 7.96.

**1,1,1-Tris[(4S)-4-benzyloxazolin-2-yl]ethane:** *t*BuLi (1.8 mL, 1.5 M in pentane, 2.6 mmol) was added dropwise to a solution of 1,1-bis[(4S)-4-benzyloxazolin-2-yl]ethane (768 mg, 2.2 mmol) in THF (80 mL) at  $-78^\circ\text{C}$ . The resulting yellow solution was stirred for an additional 30 min prior to the addition of (4S)-2-bromo-4-benzyloxazoline (1.2 equiv, 634 mg, 2.6 mmol).<sup>[39]</sup> The solution was allowed to warm slowly to room temperature over 12 h and then concentrated to remove the pentane; finally the Schlenk tube was sealed. The stirred solution was heated at  $70^\circ\text{C}$  for 3 d. The resulting orange solution was evaporated to dryness. The residue was redissolved in dichloromethane (100 mL) and washed with water (10 mL). The organic extract was dried over  $\text{Na}_2\text{SO}_4$  and concentrated in vacuo to give an orange oil. Purification by flash chromatography ( $\text{CH}_2\text{Cl}_2/\text{MeOH}/\text{Et}_3\text{N}$ , 97:3:1) gave the desired product as a white solid (620 mg, 56% yield).  $^1\text{H}$  NMR (400 MHz,  $\text{CDCl}_3$ , 296 K):  $\delta = 1.76$  (s, 3H;  $\text{CH}_3$ ), 2.68 (dd,  $J = 8.5$ , 13.7 Hz, 3H;  $\text{CH}_{2\text{Bn}}$ ), 3.11 (dd,  $J = 5.1$ , 13.7 Hz, 3H;  $\text{CH}_{2\text{Bn}}$ ), 4.07 (dd,  $J = 6.9$ , 8.3 Hz, 3H;  $\text{CH}_{2\text{oxa}}$ ), 4.23 (dd,  $J = 8.5$ , 9.0 Hz, 3H;  $\text{CH}_{2\text{oxa}}$ ), 4.46 (m, 3H;  $\text{CH}_{\text{oxa}}$ ), 7.24 ppm (m, 15H;  $\text{CH}_{\text{arom}}$ );  $^{13}\text{C}$  { $^1\text{H}$ } NMR (100 MHz,  $\text{CDCl}_3$ , 296 K):  $\delta = 20.9$  ( $\text{CH}_3$ ), 41.2 ( $\text{CH}_{2\text{Bn}}$ ), 44.6 ( $(\text{CH}_3)\text{C}(\text{oxa})_3$ ), 67.2 ( $\text{CH}_{\text{oxa}}$ ), 72.5 ( $\text{CH}_{2\text{oxa}}$ ), 126.4, 128.4, 129.4 ( $\text{C}_{\text{arom}}$ ), 137.7 ( $\text{C}_{\text{quat-arom}}$ ), 165.0 ppm (NCO); FT-IR (KBr):  $\tilde{\nu} = 1664\text{ cm}^{-1}$  (s, C=N); MS (FAB):  $m/z$  (%): 508.5 (100) [ $M^+$ ]; elemental analysis calcd (%) for  $\text{C}_{32}\text{H}_{33}\text{N}_3\text{O}_3$ : C 75.71, H 6.55, N 8.28; found: C 75.55, H 6.52, N 8.33.

#### Preparation of the palladium complexes

**[Pd(trisox)Cl<sub>2</sub>] complexes—general procedure.**<sup>[41]</sup> Bis(benzonitrile)palladium(II) dichloride (0.142 mmol) and the required trisox derivative (0.149 mmol) were dissolved in  $\text{CH}_2\text{Cl}_2$  (1 mL). The reaction mixture was stirred for 90 min at room temperature and pentane was added (8 mL) to form an orange precipitate. The crude product was washed twice with pentane (8 mL) and dried in vacuo to give the complex as an orange powder. (In the following NMR notation C = coordinated oxazoline, F = free oxazoline.)

**(1,1,1-Tris[(S)-4-isopropylloxazolin-2-yl]ethane)palladium(II) dichloride (1a):** Yield: 85%. Crystallisation from  $\text{CH}_2\text{Cl}_2/\text{Et}_2\text{O}$  gave orange crystals suitable for X-ray diffraction.  $^1\text{H}$  NMR (300 MHz,  $\text{CDCl}_3$ , 296 K):  $\delta = 0.74$  (m, 6H;  $\text{CH}(\text{CH}_3)_2$ , 2C), 0.87 (m, 9H;  $\text{CH}(\text{CH}_3)_2$ , 2C, 1F), 0.92 (d,  $J = 6.8$  Hz, 3H;  $\text{CH}(\text{CH}_3)_2$ , F), 1.81 (m, 1H;  $\text{CH}(\text{CH}_3)_2$ , F), 1.91 (s, 3H;  $\text{CH}_3$ apical), 2.87 (m, 2H;  $\text{CH}(\text{CH}_3)_2$ , C), 4.03 (m, 2H;  $\text{CH}_{2\text{oxa}}$ , F), 4.27 (m, 3H;  $\text{CH}_{2\text{oxa}}$ , C,  $\text{CH}_{\text{oxa}}$ , F), 4.44 (m, 2H;  $\text{CH}_{2\text{oxa}}$ , C), 4.66 (m, 1H;  $\text{CH}_{\text{oxa}}$ , C), 4.81 ppm (m, 1H;  $\text{CH}_{\text{oxa}}$ , C);  $^{13}\text{C}$  { $^1\text{H}$ } NMR (75 MHz,  $\text{CDCl}_3$ , 296 K):  $\delta = 13.1$ , 13.6, 17.8, 18.3, 18.5, 18.6 ( $\text{CH}(\text{CH}_3)_2$ ), 22.5 ( $\text{CH}_3$ apical), 29.3, 29.7 ( $\text{CH}(\text{CH}_3)_2$ , C), 32.1 ( $\text{CH}(\text{CH}_3)_2$ , F), 45.2 ( $(\text{CH}_3)\text{C}(\text{oxa})_3$ ), 69.3, 69.6 ( $\text{CH}_{2\text{oxa}}$ , C), 70.0, 70.4 ( $\text{CH}_{\text{oxa}}$ , C), 71.5 ( $\text{CH}_{2\text{oxa}}$ , F), 72.0 ( $\text{CH}_{\text{oxa}}$ , F), 160.1 (NCO, F), 165.8, 166.7 ppm (NCO, C);  $^{15}\text{N}$  (60 MHz,  $\text{CDCl}_3$ , 296 K):  $\delta = 160.2$ , 161.2 (N, C) 239.9 ppm (N, F); FT-IR (KBr):  $\tilde{\nu} = 1660$  (s, C=N free oxazoline), 1650  $\text{cm}^{-1}$  (s, C=N coordinated oxazoline); HRMS (ESI):  $m/z$  (%): 564.084 (85) [ $M^+ + \text{Na}$ ], 1105.177 (100) [ $2M^+ + \text{Na}$ ]; elemental analysis calcd (%) for  $\text{C}_{20}\text{H}_{33}\text{Cl}_2\text{N}_3\text{O}_3\text{Pd}$ : C 44.42, H 6.15, N 7.77; found: C 44.28, H 6.27, N 7.67.

**(1,1,1-Tris[(4R)-4-phenyloxazolin-2-yl]ethane)palladium(II) dichloride (1b):** Yield: 89%. Crystallisation from  $\text{CH}_2\text{Cl}_2/\text{pentane}$  gave orange crystals suitable for X-ray diffraction.  $^1\text{H}$  NMR (600 MHz,  $\text{CDCl}_3$ , 296 K):  $\delta = 2.27$  (s, 3H;  $\text{CH}_3$ ), 4.36 (pseudo-t,  $J = 8.4$  Hz, 1H;  $\text{CH}_{2\text{oxa}}$ , F), 4.58–4.61 (m, 2H;  $\text{CH}_{2\text{oxa}}$ , C), 4.75 (pseudo-t,  $J = 8.9$  Hz, 1H;  $\text{CH}_{2\text{oxa}}$ , C), 4.80 (pseudo-t,  $J = 9.2$  Hz, 1H;  $\text{CH}_{2\text{oxa}}$ , C), 4.90 (dd,  $J = 8.6$ , 10.2 Hz, 1H;  $\text{CH}_{2\text{oxa}}$ , F), 5.40 (dd,  $J = 8.3$ , 10.1 Hz, 1H;  $\text{CH}_{\text{oxa}}$ , F), 5.91 (dd,  $J = 2.3$ , 9.0 Hz, 1H;  $\text{CH}_{\text{oxa}}$ , C), 6.08 (dd,  $J = 3.5$ , 9.6 Hz, 1H;  $\text{CH}_{\text{oxa}}$ , C), 7.25–7.27 (m, 3H;  $\text{CH}_{\text{arom}}$ ), 7.32–7.40 ppm (m, 15H;  $\text{CH}_{\text{arom}}$ );  $^{13}\text{C}$  { $^1\text{H}$ } NMR (150 MHz,  $\text{CDCl}_3$ , 296 K):  $\delta = 22.4$  ( $\text{CH}_3$ ), 45.6 ( $(\text{CH}_3)\text{C}(\text{oxa})_3$ ), 68.5 ( $\text{CH}_{\text{oxa}}$ , C), 68.7 ( $\text{CH}_{\text{oxa}}$ , C), 69.7 ( $\text{CH}_{\text{oxa}}$ , F), 76.7 ( $\text{CH}_{2\text{oxa}}$ , F), 76.9 ( $\text{CH}_{2\text{oxa}}$ , F), 77.3 ( $\text{CH}_{2\text{oxa}}$ , C), 77.4 ( $\text{CH}_{2\text{oxa}}$ , C), 126.1, 126.6, 126.8 ( $\text{C}_{\text{arom}}$ , F), 128.3, 128.4, 128.5, 128.9, 129.0, 129.1 ( $\text{C}_{\text{arom}}$ , C), 139.4, 139.5 ( $\text{C}_{\text{quat-arom}}$ , C), 140.5 ( $\text{C}_{\text{quat-arom}}$ , F), 161.8 (NCO, NC), 167.1, 168.0 ppm (NCO, C);  $^{15}\text{N}$  (60 MHz,  $\text{CDCl}_3$ , 296 K):  $\delta = 160.8$ , 161.6 (N, C) 239.9 ppm (N, F); FT-IR (KBr):  $\tilde{\nu} = 1655\text{ cm}^{-1}$  (s, C=N); HRMS (FAB):  $m/z$  (%): 570.103 (100)

[ $M^+ - 2\text{Cl}$ ]; elemental analysis calcd (%) for  $\text{C}_{29}\text{H}_{27}\text{Cl}_2\text{N}_3\text{O}_3\text{Pd}$ : C 54.18, H 4.23, N 6.54; found: C 53.01, H 4.29, N 6.60.

**(1,1,1-Tris[(4S)-4-benzyloxazolin-2-yl]ethane)palladium(II) dichloride (1c):** Yield: 68%.  $^1\text{H}$  NMR (600 MHz,  $\text{CDCl}_3$ , 296 K):  $\delta = 1.55$  (s, 3H;  $\text{CH}_3$ ), 2.37 (pseudo-t,  $J = 11.2$  Hz, 1H;  $\text{CH}_{2\text{Bn}}$ , C), 2.79 (dd,  $J = 7.4$ , 13.9 Hz, 1H;  $\text{CH}_{2\text{Bn}}$ , F), 2.93 (dd,  $J = 8.5$ , 13.4 Hz, 1H;  $\text{CH}_{2\text{Bn}}$ , C), 3.01 (dd,  $J = 5.3$ , 13.8 Hz, 1H;  $\text{CH}_{2\text{Bn}}$ , F), 3.44 (dd,  $J = 1.4$ , 13.8 Hz, 1H;  $\text{CH}_{2\text{Bn}}$ , C), 3.82 (dd,  $J = 1.6$ , 13.2 Hz, 1H;  $\text{CH}_{2\text{Bn}}$ , F), 4.06 (pseudo-t,  $J = 8.1$  Hz, 1H;  $\text{CH}_{2\text{oxa}}$ , F), 4.17 (pseudo-t,  $J = 8.6$  Hz, 1H;  $\text{CH}_{2\text{oxa}}$ , C), 4.26 (pseudo-t,  $J = 8.8$  Hz, 1H;  $\text{CH}_{2\text{oxa}}$ , C), 4.30 (pseudo-t,  $J = 9.1$  Hz, 1H;  $\text{CH}_{2\text{oxa}}$ , F), 4.37 (dd,  $J = 1.9$ , 8.9 Hz, 1H;  $\text{CH}_{2\text{oxa}}$ , C), 4.49 (m, 1H;  $\text{CH}_{\text{oxa}}$ , F), 4.54 (dd,  $J = 1.6$ , 8.8 Hz, 1H;  $\text{CH}_{2\text{oxa}}$ , C), 5.04 (m, 1H;  $\text{CH}_{\text{oxa}}$ , C), 5.10 (m, 1H;  $\text{CH}_{\text{oxa}}$ , C), 7.19–7.24 (m, 4H;  $\text{CH}_{\text{arom}}$ ), 7.28–7.35 (m, 9H;  $\text{CH}_{\text{arom}}$ ), 7.45 ppm (m, 2H;  $\text{CH}_{\text{arom}}$ );  $^{13}\text{C}$  { $^1\text{H}$ } NMR (150 MHz,  $\text{CDCl}_3$ , 296 K):  $\delta = 20.9$  ( $\text{CH}_3$ ), 39.2, 39.4 ( $\text{CH}_{2\text{Bn}}$ , C) 40.6 ( $\text{CH}_{2\text{Bn}}$ , F) 45.0 ( $(\text{CH}_3)\text{C}(\text{oxa})_3$ ), 66.2 ( $\text{CH}_{\text{oxa}}$ , C), 67.1 ( $\text{CH}_{\text{oxa}}$ , F) 67.2 ( $\text{CH}_{\text{oxa}}$ , C), 72.8, 72.9 ( $\text{CH}_{2\text{oxa}}$ , C), 73.3 ( $\text{CH}_{2\text{oxa}}$ , F), 126.8, 127.1, 1267.3 ( $\text{C}_{\text{arom}}$ , F), 128.6, 128.7, 128.8, 129.7, 129.8, 130.1 ( $\text{C}_{\text{arom}}$ , C), 135.4, 135.9 ( $\text{C}_{\text{quat-arom}}$ , C), 136.5 ( $\text{C}_{\text{quat-arom}}$ , F), 161.0 (NCO, F), 166.6, 166.8 ppm (NCO, C);  $^{15}\text{N}$  (60 MHz,  $\text{CDCl}_3$ , 296 K):  $\delta = 161.3$ , 162.2 (N, C) 239.9 ppm (N, F); FT-IR (KBr):  $\tilde{\nu} = 1655\text{ cm}^{-1}$  (s, C=N); HRMS (FAB):  $m/z$  (%): 613.151 (100) [ $M^+ - 2\text{Cl}$ ]; elemental analysis calcd (%) for  $\text{C}_{32}\text{H}_{33}\text{Cl}_2\text{N}_3\text{O}_3\text{Pd}$ : C 56.11, H 4.86, N 6.13; found: C 56.04, H 4.80, N 6.19.

**(1,1,1-Tris[(4R,5S)-4,5-indanediylloxazolin-2-yl]ethane)palladium(II) dichloride (1d):** Yield: 73%.  $^1\text{H}$  NMR (400 MHz, 1,1,2,2- $[\text{D}_2]$ tetrachloroethane, 296 K):  $\delta = 1.50$  (s, 3H;  $\text{CH}_3$ ), 2.09 (d,  $J = 18.2$  Hz, 1H;  $\text{CH}_{2\text{Ind}}$ , C), 2.48 (d,  $J = 18.6$  Hz, 1H;  $\text{CH}_{2\text{Ind}}$ , C), 3.03 (dd,  $J = 6.8$ , 18.2 Hz, 1H;  $\text{CH}_{2\text{Ind}}$ , C), 3.08 (dd,  $J = 5.8$ , 17.8 Hz, 1H;  $\text{CH}_{2\text{Ind}}$ , C), 3.37 (m, 2H;  $\text{CH}_{2\text{Ind}}$ , F), 5.11 (ddd,  $J = 1.4$ , 5.8, 7.2 Hz, 1H;  $\text{OCH}_{\text{oxa}}$ , C), 5.15 (dd,  $J = 5.7$ , 7.2 Hz, 1H;  $\text{OCH}_{\text{oxa}}$ , C), 5.41 (dd,  $J = 5.9$ , 7.3 Hz, 1H;  $\text{OCH}_{\text{oxa}}$ , F), 5.49 (d,  $J = 7.6$  Hz, 1H;  $\text{NCH}_{\text{oxa}}$ , F), 6.25 (d,  $J = 6.8$  Hz, 1H;  $\text{NCH}_{\text{oxa}}$ , C), 6.26 (d,  $J = 6.5$  Hz, 1H;  $\text{NCH}_{\text{oxa}}$ , C), 7.16–7.46 (m, 10H;  $\text{CH}_{\text{arom}}$ ), 8.41 (m, 1H;  $\text{CH}_{\text{arom}}$ ), 8.50 ppm (m, 1H;  $\text{CH}_{\text{arom}}$ );  $^{13}\text{C}$  { $^1\text{H}$ } NMR (100 MHz, 1,1,2,2- $[\text{D}_2]$ tetrachloroethane, 296 K):  $\delta = 20.8$  ( $\text{CH}_3$ ), 37.3, 38.8, ( $\text{CH}_{2\text{Ind}}$ ), 45.2 ( $(\text{CH}_3)\text{C}(\text{oxa})_3$ ), 73.3, 74.0 ( $\text{NCH}_{\text{oxa}}$ , C), 76.4 ( $\text{NCH}_{\text{oxa}}$ , F), 85.1, 86.7, ( $\text{OCH}_{\text{oxa}}$ , C), 87.8, ( $\text{OCH}_{\text{oxa}}$ , F), 124.9, 125.0, 125.3, 125.7, 127.6, 127.9, 128.0, 128.1, 128.3, 128.9, 129.7, 129.9 ( $\text{C}_{\text{arom}}$ ), 138.2, 138.5, 138.5, 138.6 ( $\text{C}_{\text{quat-arom}}$ , C), 139.5, 140.5 ( $\text{C}_{\text{quat-arom}}$ , F), 160.3 (NCO, F), 166.6, 167.6 ppm (NCO, C);  $^{15}\text{N}$  (60 MHz, 1,1,2,2- $[\text{D}_2]$ tetrachloroethane, 296 K):  $\delta = 161.5$ , 162.8 (N, C), 238.3 ppm (N, F); FT-IR (KBr):  $\tilde{\nu} = 1653$  (s, C=N free oxazoline), 1649  $\text{cm}^{-1}$  (s, C=N coordinated oxazoline); HRMS (ESI):  $m/z$  (%): 702.035 (100) [ $M^+ + \text{Na}$ ], 644.077 [ $M^+ - \text{Cl}$ ]; elemental analysis calcd (%) for  $\text{C}_{32}\text{H}_{27}\text{Cl}_2\text{N}_3\text{O}_3\text{Pd}$ : C 56.61, H 4.01, N 6.19; found: C 56.70, H 4.18, N 6.10.

#### ( $\eta^3$ -Allyl)(1,1,1-tris[(R)-4-phenyloxazolin-2-yl]ethane)palladium(II)

**(2):**<sup>[42]</sup> Ph-trisox (65 mg, 0.14 mmol) in dry  $\text{CH}_2\text{Cl}_2$  (2 mL) was added to a solution of [ $\text{Pd}(\text{cod})(\eta^3\text{-C}_3\text{H}_5)\text{BF}_4$ ] (47.3 mg, 0.14 mmol) in dry  $\text{CH}_2\text{Cl}_2$  (1 mL). The reaction mixture was stirred for 45 min, filtered through Celite and washed with  $\text{CH}_2\text{Cl}_2$  ( $2 \times 1$  mL). The solvents were evaporated to give a white powder which was washed twice with pentane (5 mL) and dried under vacuum to yield the complex (50 mg, 52%). Suitable crystals for an X-ray diffraction study were obtained by slow diffusion of pentane into a solution of the complex in  $\text{CH}_2\text{Cl}_2$ .  $^1\text{H}$  NMR (400 MHz,  $\text{CDCl}_3$ , 296 K):  $\delta = 1.89$  (d,  $J = 12.5$  Hz, 1H;  $\text{H}_{\text{Aallyl}}$ ), 2.22 (s, 3H;  $\text{CH}_3$ ), 2.52 (d,  $J = 12.6$  Hz, 1H;  $\text{H}_{\text{Aallyl}}$ ), 2.78 (dd,  $J = 2.0$ , 7.0 Hz, 1H;  $\text{H}_{\text{Sallyl}}$ ), 3.44 (d,  $J = 6.9$  Hz, 1H;  $\text{H}_{\text{Aallyl}}$ ), 4.40 (pseudo-t,  $J = 8.3$  Hz, 3H;  $\text{CH}_{2\text{oxa}}$ ), 4.89 (m, 1H;  $\text{H}_{\text{Callyl}}$ ), 5.03 (dd,  $J = 8.7$ , 10.4 Hz, 3H;  $\text{CH}_{2\text{oxa}}$ ), 5.47 (dd,  $J = 7.9$ , 10.4 Hz, 3H;  $\text{CH}_{\text{oxa}}$ ), 7.33 ppm (m, 15H;  $\text{CH}_{\text{arom}}$ );  $^{13}\text{C}$  { $^1\text{H}$ } NMR (100 MHz,  $\text{CDCl}_3$ , 296 K):  $\delta = 20.8$  ( $\text{CH}_3$ ), 45.9 ( $(\text{CH}_3)\text{C}(\text{oxa})_3$ ), 61.1 ( $\text{C}_{1\text{allyl}}$ ,  $\text{C}_{3\text{allyl}}$ ), 71.6 ( $\text{CH}_{\text{oxa}}$ ), 77.0 ( $\text{CH}_{2\text{oxa}}$ ), 115.6 ( $\text{C}_{2\text{allyl}}$ ), 127.0, 128.6, 129.2 ( $\text{C}_{\text{arom}}$ ), 140.2 ( $\text{C}_{\text{quat-arom}}$ ), 167.6 ppm (NCO); FT-IR (KBr):  $\tilde{\nu} = 1658\text{ cm}^{-1}$  (s, C=N); MS (FAB):  $m/z$  (%): 612.1 (100) [ $M^+ - \text{BF}_4$ ]; elemental analysis calcd (%) for  $\text{C}_{32}\text{H}_{32}\text{N}_3\text{O}_3\text{PdBF}_4$  with  $\text{CH}_2\text{Cl}_2$ : C 50.51, H 4.37, N 5.35; found: C 50.47, H 4.32, N 5.41.

**[Pd(ma)(trisox)] complexes—general procedure.**<sup>[23a]</sup> Trisox (0.54 mmol) in dry THF (3 mL) was added to a solution of [ $\text{Pd}^0(\eta^2\text{-nbd})(\eta^2\text{-ma})$ ] (0.54 mmol) in dry THF (4 mL). After stirring for 15 min, the reaction mixture was filtered through Celite and concentrated under reduced

pressure to 2 mL. Pentane (10 mL) was then added to the solution, after which a yellow powder was obtained. The crude solid was washed with pentane (3 × 7 mL) and dried in vacuo to give the complex as a yellow powder.

**(1,1,1-Tris[(S)-4-isopropylloxazolin-2-yl]ethane)(maleic anhydride)palladium(0) (3a):** Yield: 54%. Crystallisation from Et<sub>2</sub>O/pentane gave yellow crystals suitable for an X-ray diffraction study. <sup>1</sup>H NMR (300 MHz, CDCl<sub>3</sub>, 296 K): δ = 0.81 (d, J = 6.8 Hz, 9H; CH(CH<sub>3</sub>)<sub>2</sub>), 0.96 (d, J = 7 Hz, 9H; CH(CH<sub>3</sub>)<sub>2</sub>), 1.85 (s, 3H; CH<sub>3</sub>apical), 2.23 (brm, 3H; CH(CH<sub>3</sub>)<sub>2</sub>), 3.69 (d, J = 3.7 Hz, 1H; C<sub>4</sub>H<sub>2</sub>O<sub>3</sub>), 3.74 (d, J = 3.7 Hz, 1H; C<sub>4</sub>H<sub>2</sub>O<sub>3</sub>), 4.20 (m, 6H; CH<sub>2</sub>oxa), 4.33 ppm (m, 3H; CH<sub>oxa</sub>); <sup>13</sup>C {<sup>1</sup>H} NMR (75 MHz, CDCl<sub>3</sub>, 296 K): δ = 14.8 (CH(CH<sub>3</sub>)<sub>2</sub>), 18.4 (CH(CH<sub>3</sub>)<sub>2</sub>), 21.9 (CH<sub>3</sub>apical), 30.5 (CH(CH<sub>3</sub>)<sub>2</sub>), 38.9 (CH<sub>ma</sub>), 40.4 (CH<sub>ma</sub>), 44.6 ((CH<sub>3</sub>)C(oxa)<sub>3</sub>), 69.5 (CH<sub>oxa</sub>), 72.8 (CH<sub>2</sub>oxa), 164.3 (NCO), 172.3 (C<sub>quat</sub>-ma), 172.8 ppm (C<sub>quat</sub>-ma); FT-IR (KBr):  $\tilde{\nu}$  = 1786, 1722 (C=O), 1660 (C=N, coordinated oxazoline), 1650 cm<sup>-1</sup> (C=N, free oxazoline); HRMS (ESI): *m/z* (%): 590.162 (100) [M<sup>+</sup>+Na], 1159.329 (12) [2M<sup>+</sup>+Na]; elemental analysis calcd (%) for C<sub>24</sub>H<sub>35</sub>Cl<sub>2</sub>N<sub>3</sub>O<sub>6</sub>Pd: C 50.75, H 6.21, N 7.40; found: C 50.86, H 6.19, N 7.37;

**(1,1,1-Tris[(R)-4-phenylloxazolin-2-yl]ethane)(maleic anhydride)palladium(0) (3b):** Yield: 75%; <sup>1</sup>H NMR (600 MHz, CD<sub>2</sub>Cl<sub>2</sub>, 296 K): δ = 2.16 (s, 3H; CH<sub>3</sub>), 2.92 (d, J = 3.9 Hz, 1H; C<sub>4</sub>H<sub>2</sub>O<sub>3</sub>), 3.30 (d, J = 3.8 Hz, 1H; C<sub>4</sub>H<sub>2</sub>O<sub>3</sub>), 4.46 (brs, 3H; CH<sub>2</sub>oxa), 4.86 (pseudo-t, J = 9.2 Hz, 3H; CH<sub>2</sub>oxa), 5.40 (dd, J = 6.7, 10.1 Hz, 3H; CH<sub>oxa</sub>), 7.33–7.48 ppm (m, 15H; CH<sub>arom</sub>); <sup>13</sup>C {<sup>1</sup>H} NMR (150 MHz, CD<sub>2</sub>Cl<sub>2</sub>, 296 K): δ = 22.2 (CH<sub>3</sub>), 38.9 (CH<sub>ma</sub>), 41.4 (CH<sub>ma</sub>), 45.6 ((CH<sub>3</sub>)C(oxa)<sub>3</sub>), 76.2 (CH<sub>2</sub>oxa), 76.6 (CH<sub>2</sub>oxa), 76.7 (CH<sub>oxa</sub>), 127.0, 127.2, 127.9, 128.7, 129.1 (C<sub>arom</sub>), 140.7 (C<sub>quat</sub>-arom), 166.5 (NCO), 171.9 (C<sub>quat</sub>-ma), 172.7 ppm (C<sub>quat</sub>-ma); FT-IR (KBr):  $\tilde{\nu}$  = 1798, 1727 (C=O), 1662 (C=N, coordinated oxazoline), 1655 cm<sup>-1</sup> (C=N, free oxazoline); HRMS (FAB): *m/z* (%): 571.114 (100) [M<sup>+</sup>-ma]; elemental analysis calcd (%) for C<sub>33</sub>H<sub>29</sub>N<sub>3</sub>O<sub>6</sub>Pd: C 59.16, H 4.36, N 6.27; found: C 58.02, H 4.32, N 6.35.

**(1,1,1-Tris[(4S)-4-benzylloxazolin-2-yl]ethane)(maleic anhydride)palladium(0) (3c):** Yield: 56%; <sup>1</sup>H NMR (400 MHz, CD<sub>2</sub>Cl<sub>2</sub>, 296 K): δ = 1.53 (s, 3H; CH<sub>3</sub>), 2.78 (dd, J = 8.1, 13.2 Hz, 2H; CH<sub>2</sub>Bn), 1H; C<sub>4</sub>H<sub>2</sub>O<sub>3</sub>), 3.13 (brm, 2H; CH<sub>2</sub>Bn), 1H; C<sub>4</sub>H<sub>2</sub>O<sub>3</sub>) 3.87 (brm, 2H; CH<sub>2</sub>Bn), 4.14 (brm, 3H; CH<sub>2</sub>oxa), 4.27 (pseudo-t, J = 8.8 Hz, 3H; CH<sub>2</sub>oxa), 4.51 (m, 3H; CH<sub>oxa</sub>), 7.22–7.34 ppm (m, 15H; CH<sub>arom</sub>); <sup>13</sup>C {<sup>1</sup>H} NMR (100 MHz, CD<sub>2</sub>Cl<sub>2</sub>, 296 K): δ = 21.8 (CH<sub>3</sub>), 39.8 (CH<sub>ma</sub>), 40.5 (CH<sub>2</sub>Bn), 41.2 (CH<sub>ma</sub>), 45.0 ((CH<sub>3</sub>)C(oxa)<sub>3</sub>), 68.2 (CH<sub>oxa</sub>), 72.8 (CH<sub>2</sub>oxa), 127.1, 128.9, 130.2 (C<sub>arom</sub>), 139.8 (C<sub>quat</sub>-arom), 164.4 (NCO), 172.8 (C<sub>quat</sub>-ma), 173.6 ppm (C<sub>quat</sub>-ma); FT-IR (KBr):  $\tilde{\nu}$  = 1793, 1724 (C=O), 1662 (C=N, coordinated oxazoline), 1655 cm<sup>-1</sup> (C=N, free oxazoline); HRMS (FAB): *m/z* (%): 614.162 (100) [M<sup>+</sup>-ma].

**(2,2-Bis[(4S)-4-isopropylloxazolin-2-yl]-1-(pyrin-2-yl)propane)(maleic anhydride)palladium(0) (3e):** Yield: 69%; <sup>1</sup>H NMR (600 MHz, CD<sub>2</sub>Cl<sub>2</sub>, 296 K): δ = 0.48–0.53 (m, 2H; CH(CH<sub>3</sub>)<sub>2</sub>), 0.74–0.98 (m, 10H; CH(CH<sub>3</sub>)<sub>2</sub>), 1.71, 173 (s, 3H; CH<sub>3</sub>apical), 2.33 (brm, 1H; CH(CH<sub>3</sub>)<sub>2</sub>), 2.45 (brm, 1H; CH(CH<sub>3</sub>)<sub>2</sub>), 3.43 (d, J = 15.2 Hz, 1H; CH<sub>2</sub>py), 3.52 (d, J = 16.1 Hz, 1H; CH<sub>2</sub>py), 3.60–3.68 (m, 2H; C<sub>4</sub>H<sub>2</sub>O<sub>3</sub>), 4.02–4.32 (m, 6H; CH<sub>2</sub>oxa, CH<sub>oxa</sub>), 7.11 (m, 2H; CH<sub>arom</sub>), 7.61 (m, 1H; CH<sub>arom</sub>), 8.41 ppm (m, 1H; CH<sub>arom</sub>); <sup>13</sup>C {<sup>1</sup>H} NMR (150 MHz, CD<sub>2</sub>Cl<sub>2</sub>, 296 K): δ = 13.6, 13.8, 18.4 (CH(CH<sub>3</sub>)<sub>2</sub>), 26.1 (CH<sub>3</sub>apical), 29.1, 29.6 (CH(CH<sub>3</sub>)<sub>2</sub>), 37.5, 39.3 (CH<sub>ma</sub>), 43.9 (CH<sub>2</sub>Bn), 42.7 ((CH<sub>3</sub>)C(oxa)<sub>3</sub>), 67.8, 68.2 (CH<sub>oxa</sub>), 72.2 (CH<sub>2</sub>oxa), 121.6, 122.8, 136.0 (C<sub>arom</sub>), 156.3 (C<sub>quat</sub>-arom), 169.1 (NCO), 172.8, 173.8 ppm (C<sub>quat</sub>-ma); FT-IR (KBr):  $\tilde{\nu}$  = 1794, 1723 (C=O), 1664 (C=N, coordinated oxazoline), 1653 cm<sup>-1</sup> (C=N free oxazoline); HRMS (FAB): *m/z* (%): 449.131 (100) [M<sup>+</sup>-ma].

**(1,1,1-Tris[(4R,5S)-4,5-indanediylloxazolin-2-yl]ethane)(tetracyanoethylene)palladium(0) (3d):** Ind-trisox (105 mg, 0.21 mmol) in THF (2 mL) was added to a solution of [Pd(η<sup>2</sup>,η<sup>2</sup>-nbd)(η<sup>2</sup>-tcne)] (68 mg, 0.21 mmol) in THF (2 mL). After stirring for 2 h, the reaction mixture was filtered through Celite and concentrated under reduced pressure to 2 mL. Pentane (10 mL) was then added to the solution, after which a yellow powder was obtained. The crude solid was washed three times with pentane (7 mL) and dried in vacuo to yield 70 mg (50%) of the complex as a yellow powder. <sup>1</sup>H NMR (400 MHz, CD<sub>2</sub>Cl<sub>2</sub>, 296 K): δ = 1.60 (s, 3H; CH<sub>3</sub>), 2.77 (d, J = 18 Hz, 3H; CH<sub>2</sub>Ind), 3.28 (dd, J = 6.4, 18.3 Hz, 3H;

CH<sub>2</sub>Ind), 5.40 (pseudo-t, J = 6.6 Hz, 3H; OCH<sub>oxa</sub>), 5.66 (d, J = 7.4 Hz, 3H; NCH<sub>oxa</sub>) 7.28 (m, 3H; CH<sub>arom</sub>), 7.38 (m, 6H; CH<sub>arom</sub>), 7.73 ppm (m, 3H; CH<sub>arom</sub>); <sup>13</sup>C NMR (100 MHz, CD<sub>2</sub>Cl<sub>2</sub>, 296 K): δ = 20.6 (CH<sub>3</sub>), 38.6 (CH<sub>2</sub>Ind), 45.6 ((CH<sub>3</sub>)C(oxa)<sub>3</sub>), 77.8 (NCH<sub>oxa</sub>), 86.9 (OCH<sub>oxa</sub>), 114.6, 115.0 (C<sub>tcne</sub>), 125.7, 126.2, 128.3, 129.8 (C<sub>arom</sub>), 139.3, 139.6 (C<sub>quat</sub>-arom), 159.7 ppm (NCO); <sup>1</sup>H NMR (400 MHz, CD<sub>2</sub>Cl<sub>2</sub>, 203 K): δ = 1.54 (s, 3H; CH<sub>3</sub>), 1.88 (d, J = 18.2 Hz, 1H; CH<sub>2</sub>Ind), 2.42 (d, J = 18.3 Hz, 1H; CH<sub>2</sub>Ind), 3.01 (dd, J = 6.8, 18.4 Hz, 1H; CH<sub>2</sub>Ind), 3.18 (dd, J = 5.2, 18.3 Hz, 1H; CH<sub>2</sub>Ind), 3.38 (d, J = 18.4 Hz, 1H; CH<sub>2</sub>Ind), 3.46 (dd, J = 5.7, 19.2 Hz, 1H; CH<sub>2</sub>Ind), 5.14 (pseudo-t, J = 7.0 Hz, 1H; OCH<sub>oxa</sub>), 5.36 (pseudo-t, J = 6.1 Hz, 1H; OCH<sub>oxa</sub>), 5.53 (d, J = 7.8 Hz, 1H; NCH<sub>oxa</sub>), 5.58 (d, J = 7.0 Hz, 1H; NCH<sub>oxa</sub>), 5.61 (pseudo-t, J = 6.4 Hz, 1H; OCH<sub>oxa</sub>), 5.76 (d, J = 7.2 Hz, 1H; NCH<sub>oxa</sub>), 7.35 (m, 10H; CH<sub>arom</sub>), 7.76 (d, J = 7.8 Hz, 1H; CH<sub>arom</sub>); 7.87 ppm (d, J = 7.5 Hz, 1H; CH<sub>arom</sub>); <sup>13</sup>C NMR (100 MHz, CD<sub>2</sub>Cl<sub>2</sub>, 203 K): δ = 20.6 (CH<sub>3</sub>), 37.1, 37.4, 38.1, 38.4 (CH<sub>2</sub>Ind), 44.3 ((CH<sub>3</sub>)C(oxa)<sub>3</sub>), 76.0, 77.0 (NCH<sub>oxa</sub>), 77.7, 84.0, 86.7 (OCH<sub>oxa</sub>), 87.0 (NCH<sub>oxa</sub>), 113.8, 114.4 (C<sub>tcne</sub>), 124.8, 125.1, 127.6, 129.5 (C<sub>arom</sub>), 137.5, 138.9 (C<sub>quat</sub>-arom), 160.2, 168.0 ppm (NCO); FT-IR (KBr):  $\tilde{\nu}$  = 1653 (C=N, coordinated oxazoline), 1649 cm<sup>-1</sup> (C=N, free oxazoline); HRMS (FAB): *m/z* (%): 607.115 (100) [M<sup>+</sup>-tcne], 735.129 (50) [M<sup>+</sup>].

**Procedure for the palladium-catalysed allylic alkylation reaction:** A degassed solution of [Pd(η<sup>3</sup>-C<sub>3</sub>H<sub>5</sub>)Cl]<sub>2</sub> (6.4 μmol, 1.1 mol%) and ligand (14.5 μmol, 2.5 mol%) in THF (0.7 mL) was stirred at 50 °C for 1.5 h. After cooling down to room temperature, *rac*-1,3-diphenylprop-2-enyl acetate (147 mg, 0.58 mmol) in THF (2.2 mL) dimethyl malonate (0.2 mL, 1.75 mmol), BSA (0.4 mL, 1.75 mmol) and a few milligrams of potassium acetate were added. The reaction mixture was stirred at room temperature. After the desired reaction time the reaction mixture was diluted with CH<sub>2</sub>Cl<sub>2</sub>, washed with a saturated aqueous solution of ammonium chloride and the organic extract was dried over Na<sub>2</sub>SO<sub>4</sub>. The residue was purified by flash chromatography and the *ee* of the product was determined by HPLC using a Daicel Chiralpak AD-H column. Yields and *ee* values are the average of at least two corroborating runs. The absolute configuration was assigned by comparing the optical rotation value with literature data.<sup>[43]</sup>

The comparative studies of the catalytic activities were conducted for each experiment using palladium catalysts prepared in situ by reacting the respective ligand with the [Pd(η<sup>3</sup>-C<sub>3</sub>H<sub>5</sub>)Cl]<sub>2</sub> dimer at 50 °C for 1.5 h in THF. The catalytic allylic alkylations were carried out at room temperature. The progress of the reaction was monitored by measuring the appearance of the product by GC, using dodecane as internal standard.

**Crystal structure determinations:** Single crystals of the complexes **1a**, **1b**, **2**, **3a** and **3b** were obtained by layering concentrated solutions in polar solvents (dichloromethane or diethyl ether) with pentane or diethyl ether and allowing slow diffusion at room temperature. Intensity data were collected at low temperature on Nonius Kappa CCD (**1a**, **3a**) and Bruker Smart 1000 CCD (**1b**, **2**, **3b**) diffractometers. Crystals of **3b**, although of nice appearance, were invariably found to be multiples. Datasets from two different crystals could only be partially de-twinned, resulting in unacceptably high *R*<sub>int</sub> values. The structure could be solved but not refined to a satisfactory level. Crystal data and experimental details are given in Table 6.

Data were corrected for Lorentz, polarisation and absorption effects (semiempirical<sup>[44]</sup> or empirical<sup>[45]</sup>). The structures were solved using heavy atom or direct methods and refined by a full-matrix least-squares procedure based on *F*<sup>2</sup> with all measured unique reflections. All non-hydrogen atoms were given anisotropic displacement parameters. Hydrogen atoms were input at calculated positions and refined with a riding model. In the structure of **2**, dichloromethane was found as a solvent of crystallisation. The calculations were performed by using the programs DIRDIF,<sup>[46]</sup> SIR,<sup>[47]</sup> SHELXS-86,<sup>[48]</sup> SHELXL-97<sup>[49]</sup> and OpenMoleN.<sup>[50]</sup> Graphical representations were drawn with XP.<sup>[51]</sup> Anisotropic displacement ellipsoids are scaled to 25% probability.

CCDC-633244 (**1a**), CCDC-633245 (**1b**), CCDC-633246 (**2**) and CCDC-633247 (**3a**) contain the supplementary crystallographic data for this paper. These data can be obtained free of charge from The Cambridge Crystallographic Data Centre via [www.ccdc.cam.ac.uk/data\\_request/cif](http://www.ccdc.cam.ac.uk/data_request/cif).

Table 6. X-ray experimental data of the crystallographically characterised compounds.

	<b>1a</b>	<b>1b</b>	<b>2</b>	<b>3a</b>
formula	C <sub>20</sub> H <sub>35</sub> Cl <sub>2</sub> N <sub>3</sub> O <sub>3</sub> Pd	C <sub>20</sub> H <sub>27</sub> Cl <sub>2</sub> N <sub>3</sub> O <sub>3</sub> Pd	C <sub>33</sub> H <sub>34</sub> BCl <sub>2</sub> F <sub>4</sub> N <sub>3</sub> O <sub>3</sub> Pd	C <sub>24</sub> H <sub>35</sub> N <sub>3</sub> O <sub>6</sub> Pd
<i>M</i> <sub>r</sub>	540.81	642.84	784.74	567.96
<i>T</i> [K]	173	100(2)	100(2)	173
crystal system	orthorhombic	monoclinic	monoclinic	monoclinic
space group	<i>P</i> 2 <sub>1</sub> 2 <sub>1</sub> 2 <sub>1</sub>	<i>P</i> 2 <sub>1</sub>	<i>P</i> 2 <sub>1</sub>	<i>P</i> 2 <sub>1</sub>
<i>a</i> [Å]	8.7083(1)	10.2954(10)	9.1344(4)	10.4450(2)
<i>b</i> [Å]	10.8395(1)	10.0926(10)	20.6281(10)	10.0975(2)
<i>c</i> [Å]	24.8911(4)	13.0348(13)	9.3599(4)	14.0887(3)
$\beta$ [°]		101.537(2)	111.4780(10)	90.161(5)
<i>V</i> [Å <sup>3</sup> ]	2349.56(5)	1327.0(2)	1641.17(13)	1485.91(5)
<i>Z</i>	4	2	2	2
$\rho_{\text{calcd}}$ [Mg m <sup>-3</sup> ]	1.53	1.609	1.588	1.27
$\mu$ [mm <sup>-1</sup> ]	1.042	0.938	0.790	0.661
<i>F</i> <sub>000</sub>	1112	652	796	588
crystal size [mm <sup>3</sup> ]	0.10 × 0.06 × 0.06	0.20 × 0.05 × 0.05	0.30 × 0.30 × 0.30	0.20 × 0.16 × 0.10
$\theta$ range [°]	2.5–30.02	2.02–32.08	1.97–32.01	2.5–30.05
index ranges	–12 ≤ <i>h</i> ≤ 12 –15 ≤ <i>k</i> ≤ 15 –34 ≤ <i>l</i> ≤ 35	–15 ≤ <i>h</i> ≤ 14 –14 ≤ <i>k</i> ≤ 15 0 ≤ <i>l</i> ≤ 19	–13 ≤ <i>h</i> ≤ 12 –30 ≤ <i>k</i> ≤ 25 0 ≤ <i>l</i> ≤ 13	–14 ≤ <i>h</i> ≤ 14 –14 ≤ <i>k</i> ≤ 14 –19 ≤ <i>l</i> ≤ 19
reflms collected		32759	15547	8556
independent reflms [ <i>R</i> <sub>int</sub> ]	6871 [0.040]	8646 [0.0583]	8670 [0.0224]	4588 [0.040]
completeness to $\theta = 30.02^\circ$ [%]	99.9	95.6	100	99.8
absorption correction	empirical (SHELXA)	semi-empirical from equivalents	semi-empirical from equivalents	empirical (SHELXA)
max/min transmission	0.928/0.901	0.7458/0.6070	0.7974/0.7974	1.0000/0.9401
data/restraints/parameters	4997/0/262	8646/1/344	8670/8/43	3495/1/306
goodness-of-fit on <i>F</i> <sup>2</sup>	1.323	1.084	1.072	1.966
final <i>R</i> indices [ <i>I</i> > 2 $\sigma$ ( <i>I</i> )]	<i>R</i> 1 = 0.033, <i>wR</i> 2 = 0.037	<i>R</i> 1 = 0.0372, <i>wR</i> 2 = 0.0688	<i>R</i> 1 = 0.0290, <i>wR</i> 2 = 0.0748	<i>R</i> 1 = 0.038, <i>wR</i> 2 = 0.061
<i>R</i> indices (all data)	<i>R</i> 1 = 0.058, <i>wR</i> 2 = 0.108	<i>R</i> 1 = 0.0560, <i>wR</i> 2 = 0.0750	<i>R</i> 1 = 0.0303, <i>wR</i> 2 = 0.0760	<i>R</i> 1 = 0.051, <i>wR</i> 2 = 0.120
Abs. struct. parameter	–0.02(3)	0.000(19)	–0.021(15)	–0.04(3)
Res. density, max diff. peak/hole [e Å <sup>-3</sup> ]	1.115/–0.304	1.430/–0.609	1.218/–0.603	0.895/–0.317

## Acknowledgements

We thank the Deutsche Forschungsgemeinschaft (SFB 623), the CNRS (France) and the Deutsch-Französische Hochschule for funding. Support by BASF (Ludwigshafen) and Degussa (Hanau) is gratefully acknowledged. We also thank Dr A. De Cian and N. Gruber for some of the X-Ray diffraction studies.

- [1] a) C. Moberg, *Angew. Chem.* **1998**, *110*, 260; *Angew. Chem. Int. Ed.* **1998**, *37*, 248; b) M. C. Keyes, W. B. Tolman, *Adv. Catal. Processes* **1997**, *2*, 189.
- [2] a) S. E. Gibson, M. P. Castaldi, *Chem. Commun.* **2006**, 3045; b) S. E. Gibson, M. P. Castaldi, *Angew. Chem.* **2006**, *118*, 4834; *Angew. Chem. Int. Ed.* **2006**, *45*, 4718; c) C. Moberg, *Angew. Chem.* **2006**, *118*, 4838; *Angew. Chem. Int. Ed.* **2006**, *45*, 4721.
- [3] Examples of the use of C<sub>3</sub>-chiral ligands in asymmetric catalysis: a) H. Brunner, A. F. M. M. Rahman, *Chem. Ber.* **1984**, *117*, 710; b) M. J. Burk, R. L. Harlow, *Angew. Chem.* **1990**, *102*, 1511; *Angew. Chem. Int. Ed. Engl.* **1990**, *29*, 1467; c) M. J. Burk, J. E. Feaster, R. L. Harlow, *Tetrahedron: Asymmetry* **1991**, *2*, 569; d) T. R. Ward, L. M. Venanzi, A. Albinati, F. Lianza, T. Gerfin, V. Gramlich, G. M. R. Tombo, *Helv. Chim. Acta* **1991**, *74*, 983; e) M. J. Baker, P. J. Pringle, *J. Chem. Soc. Chem. Commun.* **1993**, 314; f) H. Adolfsson, K. Wärnmark, C. Moberg, *J. Chem. Soc. Chem. Commun.* **1992**, 1054; g) H. Adolfsson, K. Nordström, K. Wärnmark, C. Moberg, *Tetrahedron: Asymmetry* **1996**, *7*, 1967; h) D. D. LeCloux, W. B. Tolman, *J. Am. Chem. Soc.* **1993**, *115*, 1153; i) C. J. Tokar, P. B. Kettler, W. B. Tolman, *Organometallics* **1992**, *11*, 2737; j) D. D. LeCloux, C. J. Tokar, M. Osawa, R. P. Houser, M. C. Keyes, W. B. Tolman, *Organometallics* **1994**, *13*, 2855; k) K. Kawasaki, S. Tsumura, T. Katsuki, *Synlett* **1995**, 1245.

- [4] Asymmetric catalysis with chiral aminoalcohols as ligands: a) W. A. Nugent, R. L. Harlow, *J. Am. Chem. Soc.* **1994**, *116*, 6142; b) F. Di Furia, G. Licini, G. Modena, R. Motterle, W. A. Nugent, *J. Org. Chem.* **1996**, *61*, 5175; c) H. Lütjens, P. Knochel, *Tetrahedron: Asymmetry* **1994**, *5*, 1161; d) H. Lütjens, G. Wahl, F. Möller, F. Knochel, J. Sundermeyer, *Organometallics* **1997**, *16*, 5869; e) M. Cernerud, H. Adolffson, C. Moberg, *Tetrahedron: Asymmetry* **1997**, *8*, 2655; f) W. A. Nugent, G. Licini, M. Bonchio, O. Bortolini, M. G. Finn, B. W. McClelland, *Pure Appl. Chem.* **1998**, *70*, 1041; g) M. Bonchio, G. Licini, F. Di Furia, S. Mantovani, G. Modena, W. A. Nugent, *J. Org. Chem.* **1999**, *64*, 1326; h) M. Bonchio, G. Licini, G. Modena, O. Bortolini, S. Moro, W. A. Nugent, *J. Am. Chem. Soc.* **1999**, *121*, 6258; i) M. Bonchio, O. Bortolini, G. Licini, S. Moro, W. A. Nugent, *Eur. J. Org. Chem.* **2003**, 507; j) M. G. Buonomenna, E. Drioli, W. A. Nugent, L. J. Prins, P. Scrimin, G. Licini, *Tetrahedron Lett.* **2004**, *45*, 7515.
- [5] Recent advances in the design of C<sub>3</sub>-chiral podands: a) G. Bringmann, M. Breuning, R.-M. Pfeifer, P. Schreiber, *Tetrahedron: Asymmetry* **2003**, *14*, 2225; b) G. Bringmann, R.-M. Pfeifer, C. Rummey, K. Hartner, M. Breuning, *J. Org. Chem.* **2003**, *68*, 6859; c) T. Fang, D.-M. Du, S.-F. Lu, J. Xu, *Org. Lett.* **2005**, *7*, 2081; d) M. P. Castaldi, S. E. Gibson, M. Rudd, A. J. P. White, *Angew. Chem.* **2005**, *117*, 3498; *Angew. Chem. Int. Ed.* **2005**, *44*, 3432; e) M. P. Castaldi, S. E. Gibson, M. Rudd, A. J. P. White, *Chem. Eur. J.* **2006**, *12*, 138.
- [6] For a discussion of the special case of five-coordinate complexes bearing C<sub>3</sub>-chiral tripods, see: L. H. Gade, P. Renner, H. Memmler, F. Fecher, C. H. Galka, M. Laubender, S. Radojevic, M. McPartlin, J. W. Lauher, *Chem. Eur. J.* **2001**, *7*, 2563.
- [7] H. B. Kagan, T.-P. Dang, *J. Am. Chem. Soc.* **1972**, *94*, 6429.
- [8] A. von Zelewsky, *Stereochemistry of Coordination Compounds*, Wiley, Chichester, **1996**.
- [9] a) S. Bellemin-Laponnaz, L. H. Gade, *Chem. Commun.* **2002**, 1286; b) S. Bellemin-Laponnaz, L. H. Gade, *Angew. Chem.* **2002**, *114*,

- 3623; *Angew. Chem. Int. Ed.* **2002**, *41*, 3473; c) L. H. Gade, G. Marconi, C. Dro, B. D. Ward, M. Poyatos, S. Bellemin-Lapponnaz, H. Wadepohl, L. Sorace, G. Poneti, *Chem. Eur. J.* **2007**, *13*, 3058.
- [10] C. Foltz, B. Stecker, G. Marconi, H. Wadepohl, S. Bellemin-Lapponnaz, L. H. Gade, *Chem. Commun.* **2005**, 5115.
- [11] a) B. M. Trost, P. E. Strege, *J. Am. Chem. Soc.* **1977**, *99*, 1649; the first asymmetric allylic alkylation was reported four years earlier: b) B. M. Trost, T. J. Dietsche, *J. Am. Chem. Soc.* **1973**, *95*, 8200.
- [12] a) B. M. Trost, D. L. Van Vranken, *Chem. Rev.* **1996**, *96*, 395; b) A. Heumann in *Transition Metals for Organic Synthesis*, 2nd ed. (Eds.: M. Beller, C. Bolm), Wiley-VCH, Weinheim, **2004**, p. 307; c) J.-F. Paquin; M. Leutens, *Compr. Asymmetric Catal. Suppl.* **2004**, *2*, 73; d) G. Helmchen, M. Ernst, G. Paradies, *Pure Appl. Chem.* **2004**, *76*, 495; e) T. Graening, H.-G. Schmalz, *Angew. Chem.* **2003**, *115*, 2684; *Angew. Chem. Int. Ed.* **2003**, *42*, 2580; f) C. Moberg, U. Bremberg, K. Hallman, M. Svensson, P.-O. Norrby, A. Hallberg, M. Larhed, I. Csoregh, *Pure Appl. Chem.* **1999**, *71*, 1477.
- [13] a) B. M. Trost in *Catalytic Asymmetric Synthesis* (Ed.: I. Ojima), Wiley-VCH, Weinheim, **2000**, Chapter 8E; b) B. M. Trost, M. R. Machacek, A. Aponick, *Acc. Chem. Res.* **2006**, *39*, 747.
- [14] a) A. Togni, L. M. Venanzi, *Angew. Chem.* **1994**, *106*, 517; *Angew. Chem. Int. Ed. Engl.* **1994**, *33*, 497; b) B. M. Trost, C. Lee, *Catalytic Asymmetric Synthesis*, 2nd ed. (Ed.: I. Ojima), Wiley-VCH, Weinheim **2000**; c) R. Prétôt, G. C. Lloyd-Jones, A. Pfaltz, *Pure Appl. Chem.* **1998**, *70*, 1035; d) T. Hayashi, *J. Organomet. Chem.* **1999**, *576*, 195; e) G. Helmchen, *J. Organomet. Chem.* **1999**, *576*, 203; f) G. Helmchen, A. Pfaltz, *Acc. Chem. Res.* **2000**, *33*, 336.
- [15] This sidearm strategy has been successfully employed for the development of efficient ligands for a range of copper-catalysed enantioselective reactions: a) J. Zhou, M. C. Ye, Y. Tang, *J. Comb. Chem.* **2004**, *6*, 301; b) Z.-Z. Huang, Y.-B. Kang, J. Zhou, M.-C. Ye, Y. Tang, *Org. Lett.* **2004**, *6*, 1677; c) M.-C. Ye, J. Zhou, Y. Tang, *J. Org. Chem.* **2006**, *71*, 3576.
- [16] For a review see: J. Zhou, Y. Tang, *Chem. Soc. Rev.* **2005**, *34*, 664.
- [17] A. El Hatimi, M. Gómez, S. Jansat, G. Muller, M. Font-Bardía, X. Solans, *J. Chem. Soc. Dalton Trans.* **1998**, 4229.
- [18] H. M. McConnell, *J. Chem. Phys.* **1958**, *28*, 430.
- [19] M. L. H. Green, L.-L. Wong, A. Sella, *Organometallics* **1992**, *11*, 2660.
- [20] a) J. B. Goddard, F. Basolo, *Inorg. Chem.* **1968**, *7*, 936; b) L. A. P. Kane-Maguire, G. Thomas, *J. Chem. Soc. Dalton Trans.* **1975**, *19*, 1890. Studies published more recently include: c) T. Shi, L. I. Elding, *Inorg. Chem.* **1996**, *35*, 735; d) T. Shi, L. I. Elding, *Inorg. Chem.* **1997**, *36*, 528; e) Z. D. Bugarèic, G. Liehr, R. van Eldik, *J. Chem. Soc. Dalton Trans.* **2002**, 951.
- [21] a) O. Hoarau, H. Ait-Haddou, J.-C. Daran, D. Cramailere, G. G. A. Balavoine, *Organometallics* **1999**, *18*, 4718; b) M. Kehnder, M. Neuburger, P. von Matt, A. Pfaltz, *Acta Crystallogr. Sect. C* **1995**, *51*, 1109.
- [22] M. A. Pericas, C. Puigjamer, A. Riera, A. Vidal-Ferran, M. Gomez, F. Jimenez, G. Muller, M. Rocamora, *Chem. Eur. J.* **2002**, *8*, 4164 and refs cited therein.
- [23] a) A. M. Kluwer, C. J. Elsevier, M. Bühl, M. Lutz, A. L. Spek, *Angew. Chem.* **2003**, *115*, 3625; *Angew. Chem. Int. Ed.* **2003**, *42*, 3501; b) B. Crociani, F. Di Bianca, P. Uguagliati, L. Canovese, A. Berton, *J. Chem. Soc. Dalton Trans.* **1991**, *71*; c) K. J. Cavell, D. J. Stufkens, K. Vrieze, *Inorg. Chim. Acta* **1981**, *47*, 67; d) M. W. van Laren, C. J. Elsevier, *Angew. Chem.* **1999**, *111*, 3926; *Angew. Chem. Int. Ed.* **1999**, *38*, 3715; e) R. A. Klein, P. Witte, R. Van Belzen, J. Fraanje, K. Goubitz, M. Numan, H. Schenk, J. M. Ernsting, C. J. Elsevier, *Eur. J. Inorg. Chem.* **1998**, 319; f) B. Milani, A. Anzilutti, L. Vicentini, A. Sessanta o Santi, E. Zangrando, S. Geremia, G. Mestroni, *Organometallics* **1997**, *16*, 5064; g) A. M. Kluwer, T. S. Koblenz, T. Jonischkeit, K. Woelk, C. J. Elsevier, *J. Am. Chem. Soc.* **2005**, *127*, 15470.
- [24] K. Itoh, F. Ueda, K. Hirai, Y. Ishii, *Chem. Lett.* **1977**, 877.
- [25] a) D. D. Ellis, A. L. Spek, *Acta Crystallogr. Sect. C* **2001**, *57*, 235; b) J. J. M. de Pater, D. S. Tromp, D. M. Tooke, A. L. Spek, B.-J. Deelman, G. van Koten, C. J. Elsevier, *Organometallics* **2005**, *24*, 6411.
- [26] a) T. Schleis, J. Heinemann, T. P. Spaniol, R. Mülhaupt, J. Okuda, *Inorg. Chem. Commun.* **1998**, *1*, 431; b) M. L. Ferrara, F. Giordana, I. Orabona, A. Panunzi, F. Ruffo, *Eur. J. Inorg. Chem.* **1999**, 1939.
- [27] M. Lutz, *Acta Crystallogr. Sect. E* **2001**, *57*, o1136.
- [28] R. Fernandez-Galan, F. A. Jalon, B. R. Manzano, J. Rodriguez-de la Fuente, *Organometallics* **1997**, *16*, 3758.
- [29] R. Van Asselt, C. J. Elsevier, W. J. J. Smeets, A. L. Spek, *Inorg. Chem.* **1994**, *33*, 1521.
- [30] B. M. Trost, S. J. Brickner, *J. Am. Chem. Soc.* **1983**, *105*, 568.
- [31] P. von Matt, G. C. Lloyd-Jones, A. B. E. Minidis, A. Pfaltz, L. Macko, M. Neuburger, M. Zehnder, H. Rüeger, P. S. Pregosin, *Helv. Chim. Acta* **1995**, *78*, 265.
- [32] We have observed a similar behaviour for related allylic substitutions which will be reported elsewhere.
- [33] A. Abiko, S. Masamune, *Tetrahedron Lett.* **1992**, *33*, 5517.
- [34] J. Bourguignon, U. Bremberg, G. Dupas, K. Hallman, L. Hagberg, L. Hortala, V. Levacher, S. Lutsenko, E. Macedo, C. Moberg, G. Quéguiner, F. Rahm, *Tetrahedron* **2003**, *59*, 9583.
- [35] W. R. Leonard, J. L. Romine, A. I. Meyers, *J. Org. Chem.* **1991**, *56*, 1961.
- [36] D. M. Barnes, J. Ji, M. G. Fickes, M. A. Fitzgerald, S. A. King, H. E. Morton, F. A. Plagge, M. Preskill, S. H. Wagaw, S. J. Wittenberger, J. Zhang, *J. Am. Chem. Soc.* **2002**, *124*, 13097.
- [37] D. A. White, *Inorg. Synth.* **1972**, *13*, 55.
- [38] M. Honma, T. Sawada, Y. Fujisawa, M. Utsugi, H. Wanatabe, A. Umino, T. Matsamura, T. Hagihara, M. Takano, M. Nakada, *J. Am. Chem. Soc.* **2003**, *125*, 2860.
- [39] a) A. I. Meyers, K. A. Novachek, *Tetrahedron Lett.* **1996**, *37*, 1747; b) C. Foltz, S. Bellemin-Lapponnaz, L. H. Gade, unpublished results.
- [40] M. Seitz, C. Capacchione, S. Bellemin-Lapponnaz, H. Wadepohl, B. D. Ward, L. H. Gade, *Dalton Trans.* **2006**, 193.
- [41] S. E. Denmark, R. A. Stavenger, A.-M. Faucher, J. P. Edwards, *J. Org. Chem.* **1997**, *62*, 3375.
- [42] D. Franco, M. Gomez, F. Jiménez, G. Muller, M. Rocamora, M. A. Maestro, J. Mahia, *Organometallics* **2004**, *23*, 3197.
- [43] J. Sprinz, G. Helmchen, *Tetrahedron Lett.* **1993**, *34*, 1769.
- [44] G. M. Sheldrick, SADABS-2004/1, Bruker AXS, **2004**.
- [45] N. Walker, D. Stuart, *Acta Crystallogr. Sect. A* **1983**, *39*, 158.
- [46] P. T. Beurskens, G. Beurskens, R. de Gelder, S. Garcia-Granda, R. O. Gould, R. Israel, J. M. M. Smits, *DIRDIF-99*, University of Nijmegen, The Netherlands, **1999**.
- [47] M. C. Burla, M. Camalli, G. Cascarano, C. Giacovazzo, G. Polidori, R. Spagna, D. Viterbo, *J. Appl. Crystallogr.* **1989**, *22*, 389.
- [48] G. M. Sheldrick, SHELXS-86, University of Göttingen, **1986**; G. M. Sheldrick, *Acta Crystallogr. Sect. A* **1990**, *46*, 467.
- [49] G. M. Sheldrick, SHELXL-97, University of Göttingen, **1997**.
- [50] OpenMoleN, Interactive Intelligent Structure Solution, Nonius B. V., Delft, **1997**.
- [51] SHELXTL, Bruker AXS GmbH, Karlsruhe, **1997**.

Received: February 23, 2007  
Published online: May 24, 2007